

PART II

**IMPLEMENTATION OF THE DIRECT DISPLACEMENT-
BASED DESIGN METHOD FOR SEISMIC DESIGN OF
HIGHWAY BRIDGES**

Vinicio A. Suarez and Mervyn J. Kowalsky

Department of Civil, Construction and Environmental Engineering, North Carolina State
University, Campus-Box 7908, Raleigh, NC-27695, USA

ABSTRACT

This paper presents the DDBD method with all the details required for its application to the design of conventional highway bridges. The method presented here includes new features such as: the incorporation of the displacement capacity of the superstructure as a design parameter, the determination of a stability-based target displacement for piers the design of skewed bents and abutments, among others.

1. INTRODUCTION

After the Loma Prieta earthquake in 1989, extensive research has been conducted to develop improved seismic design criteria for bridges, emphasizing the use of displacements rather than forces as a measure of earthquake demand and damage in bridges. (Priestley, 1993; ATC, 1996; Caltrans, 2006; ATC, 2003; Imbsen, 2007)

Several Displacement Based Design (DBD) methodologies have been proposed. Among them, the Direct Displacement-Based Design Method (DDBD) (Priestley, 1993) has proven to be effective for performance-based seismic design of bridges, buildings and other types of structures (Priestley et al, 2007). Specific research on DDBD of bridges has focused on design of bridge piers (Kowalsky, 1995), drilled shaft bents with soil-structure interaction (Suarez and Kowalsky, 2007) and multi-span continuous bridges (Calvi and Kingsley, 1997; Kowalsky 2002; Dwairi, 2005; Ortiz, 2006).

DDBD differs from other DBD procedures for bridges, such as the Seismic Design Criteria of Caltrans (2005) or the newly proposed AASHTO Guide Specification for LRFD Seismic Bridge Design (Imbsen, 2007), in the use of an equivalent linearization approach and in its execution. While the other methods are iterative and require strength to be assumed at the beginning of the process, DDBD directly returns the strength required by the structure to meet a predefined target performance.

The purpose of this report is to present the DDBD method with all the details required for its application to the design of conventional highway bridges. The method presented here includes new features such as: the incorporation of the displacement capacity of the superstructure as a design parameter, the determination of a stability-based target displacement for piers, the design of skewed bents and abutments, among others.

2. FUNDAMENTALS OF DDBD

DDBD was first proposed by Priestley (1993) as a tool for Performance-Based Seismic Engineering. The method allows designing a structure to meet any level of performance when subjected to any level of seismic hazard. DDBD starts with the definition of a target displacement and returns the strength required to meet the target displacement under the

design earthquake. The target displacement can be selected on the basis of material strains, drift or displacement ductility, either of which is correlated to a desired damage level or limit state. For example, in the case of a bridge column, designing for a serviceability limit state could imply steel strains to minimize residual crack widths that require repair or concrete compression strains consistent with incipient crushing.

DDBD uses an equivalent linearization approach (Shibata and Sozen, 1976) by which, a nonlinear system at maximum response, is substituted by an equivalent elastic system. This system has secant stiffness, K_{eff} , and equivalent viscous damping, ξ_{eq} , to match the maximum response of the nonlinear system (Fig 1). In the case of multi degree of freedom systems, the equivalent system is a Single Degree of Freedom (SDOF) with a generalized displacement, Δ_{sys} , and the effective mass, M_{EFF} , computed with Eq. 1 and Eq. 2 respectively (Fig.2) (Calvi and Kingsley, 1995). In these equations, $\Delta_1 \dots \Delta_i \dots \Delta_n$ are the displacements of the piers and abutments (if present) according to the assumed displacement profile, and $M_1 \dots M_i \dots M_n$ are effective masses lumped at the location of piers and abutments (if present).

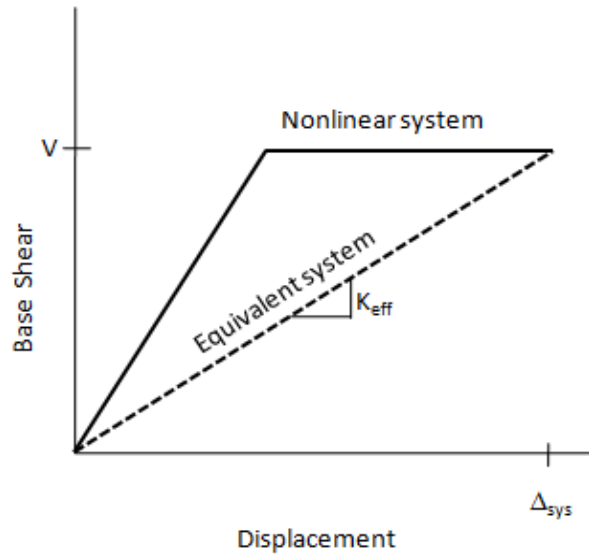


Figure 1 – Equivalent linearization approach used in DDBD

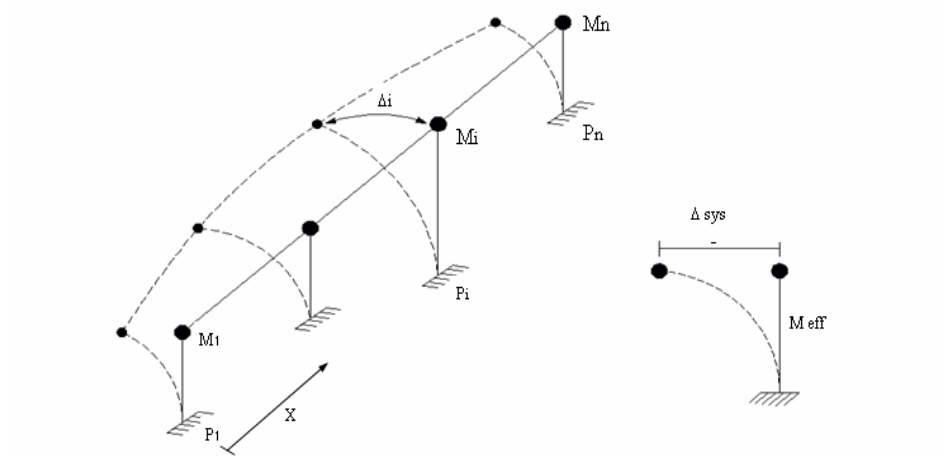


Figure 2 - Equivalent single degree of system.

$$\Delta_{sys} = \frac{\sum_{i=1}^{i=n} \Delta_i^2 M_i}{\sum_{i=1}^{i=n} \Delta_i M_i} \quad (1)$$

$$M_{eff} = \frac{\left(\sum_{i=1}^{i=n} \Delta_i M_i \right)^2}{\sum_{i=1}^{i=n} \Delta_i^2 M_i} \quad (2)$$

The energy dissipated by inelastic behavior in the bridge is accounted for in the substitute elastic system by the addition of equivalent viscous damping ξ_{eq} . With the seismic hazard represented by a displacement design spectrum that has been reduced to the level of damping in the bridge, the required effective period, T_{eff} , is easily found by entering in the displacement spectrum curve with Δ_{sys} (Fig. 3). Once T_{eff} is known, the stiffness, K_{eff} , and required strength, V , for the structure are computed from the well known relation between period, mass and stiffness for SDOF systems. Finally, V is distributed among the elements that form the earthquake resisting system, and the elements are designed and detailed following capacity design principles to avoid the formation of unwanted mechanisms.

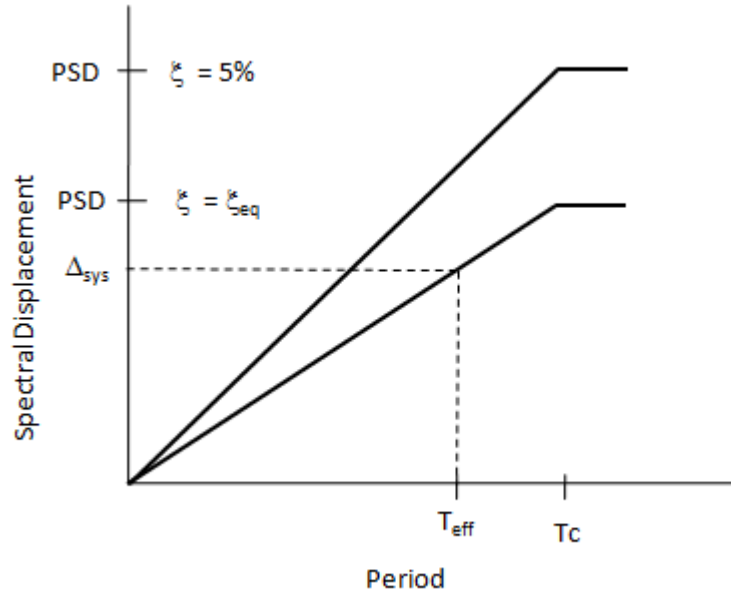


Figure 3 – Determination of effective period in DDBD

2.1 Equivalent damping

Several studies have been performed to obtain equivalent damping models suitable for DDBD (Dwairi 2005, Blandon 2005, Suarez 2006, Priestley et al 2007). These models relate equivalent damping to displacement ductility in the structure.

For reinforced concrete columns supported on rigid foundations, ξ_{eq} , is computed with Eq. 3 (Priestley, 2007).

$$\xi_{eq} = 5 + 44.4 \frac{\mu_t - 1}{\pi \mu_t} \quad (\text{Eq. 3})$$

For extended drilled shaft bents embedded in soft soils, the equivalent damping is computed by combination of hysteretic damping, $\xi_{eq,h}$, and tangent stiffness proportional viscous damping, ξ_v , with Eq. 4 (Priestley and Grant, 2005). The hysteretic damping is computed with Eq. 5 as a function of the ductility in the drilled shaft. The values of the

parameters p and q are given in Table 1 for different types of soils and boundary conditions (Suarez 2005). In Table 1, clay-20 and clay-40 refer to saturated clay soils with shear strengths of 20 kPa and 40 kPa respectively. Sand-30 and Sand-37 refer to saturated sand with friction angles of 30 and 37 degrees respectively. A fixed head implies that the head of the extended drilled shaft displaces laterally without rotation, causing double bending in the element. A pinned head implies lateral displacement with rotation and single bending. To use Eq. 4, ξ_v should be taken as 5%, since this value is typically used as default to develop design spectra.

$$\xi_{eq} = \xi_v \mu^{-0.378} + \xi_{eq,h} \quad \mu \geq 1 \quad (\text{Eq. 4})$$

$$\xi_{eq,h} = p + q \frac{\mu - 1}{\mu} \quad \mu \geq 1 \quad (\text{Eq. 5})$$

Table 1. Parameters for hysteretic damping models in drilled shaft - soil systems

HEAD	SOIL	p	q
Fixed	Clay-20	6.70	8.10
Fixed	Clay-40	5.60	8.70
Fixed	Sand-30	2.40	10.20
Fixed	Sand-37	2.00	9.60
Pinned	Clay-20	15.80	9.40
Pinned	Clay-40	13.70	10.90
Pinned	Sand-30	9.40	11.20
Pinned	Sand-37	8.50	10.40

All damping models are plotted in Fig. 4. It is observed that when ductility equals one, the equivalent damping for the column on rigid foundation equals 5% (i.e. the elastic viscous damping level) whereas the equivalent damping for the drilled shafts is higher than 5%. The additional damping comes from the soil which performs inelastically and dissipates energy at displacements that are less than the yield displacement of the reinforced concrete section. In cases where the target displacement is less than the yield displacement of the element, a linear relation between damping and ductility is appropriate. Such relation is given by Eq. 6.

$$\xi_{eq} = \xi_v + (q - \xi_v) \mu \quad \mu < 1 \quad (\text{Eq. 6})$$

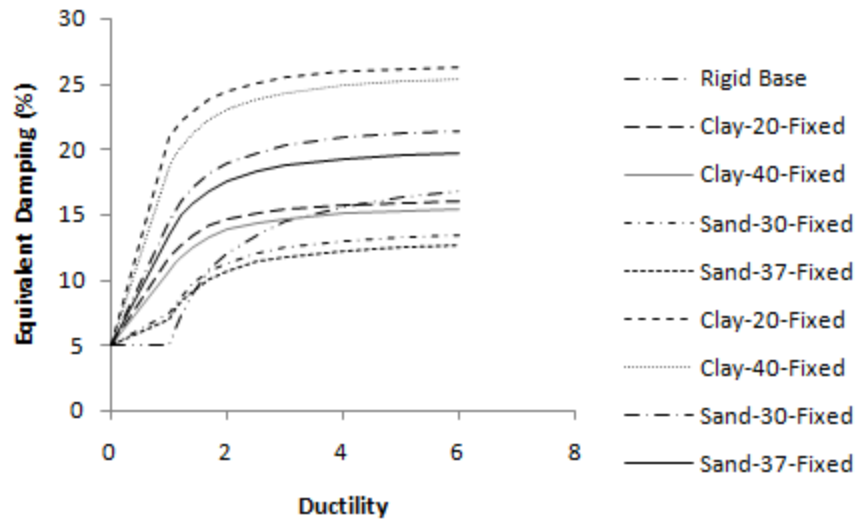


Figure 4. Equivalent damping models for bridge piers

3. GENERAL DDBD PROCEDURE FOR BRIDGES

The main steps of the design procedure are presented in Fig. 5. The bridge is previously designed for non-seismic loads and the configuration, superstructure section and foundation are known. A design objective is proposed by defining the expected performance and the seismic hazard. Then, the target displacement profile for the bridge is determined, and DDBD is applied in the longitudinal and transverse axes of the bridge. Finally the results are combined, P- Δ effects are checked and reinforcement is designed and detailed following Capacity Design principles (Priestley et al, 2007).

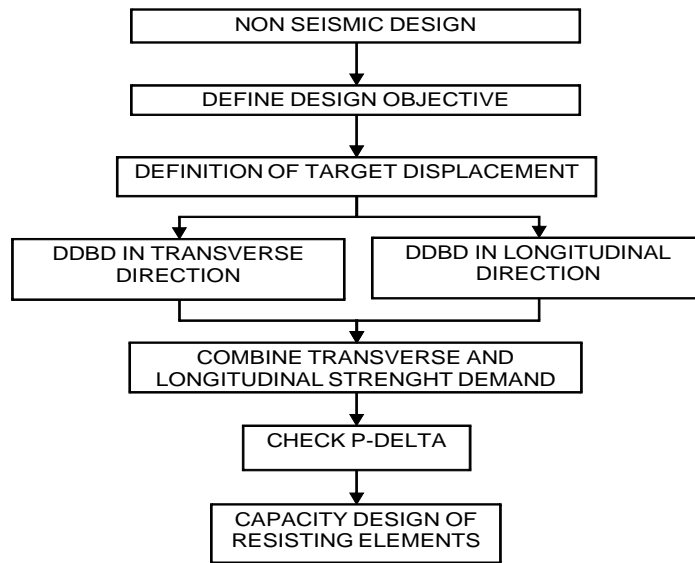


Figure 5 - DDBD main steps flowchart

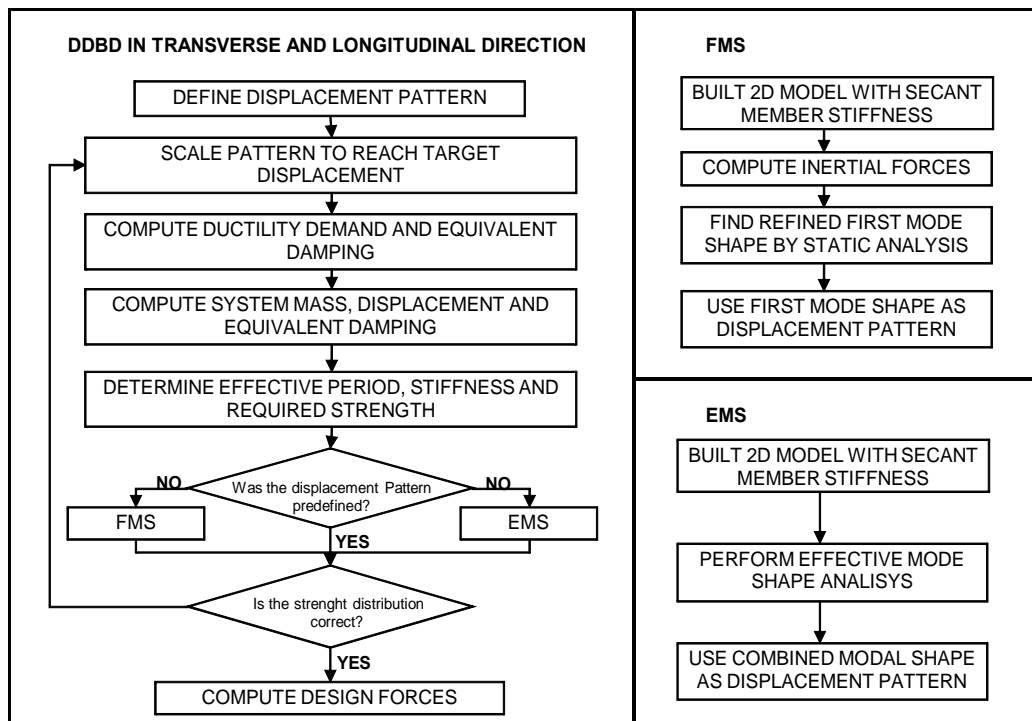



Figure 6 - Complementary DDBD flowcharts

The flowcharts in Fig. 6 show the procedure for DDBD in the transverse and longitudinal direction, as part of the general procedure shown in Fig. 5. As seen in Fig. 6, there are three

variations of the procedure: (1) If the displacement pattern is known and predefined, DDBD is applied directly; (2) If the pattern is unknown but dominated by the first mode of vibration, as in the case of bridges with integral or other type of strong abutment, a First Mode Shape (FMS) iterative algorithm is applied; (3) If the pattern is unknown but dominated by modal combination, an Effective Mode Shape (EMS) iterative algorithm is applied. The direct application of DDBD, when the displacement pattern is known, requires less effort than the application of the FMS or EMS algorithms. Recent research by the author (Suarez and Kowalsky, 2008a) showed that predefined displacement patterns can be effectively used for design of bridge frames, bridges with seat-type or other type of weak abutments and bridges with one or two expansion joints. These bridges must have a balanced distribution of mass and stiffness, according to AASHTO (Ibsen, 2007). A summary of the design algorithms applicable to common types of highway bridges is presented in Table 2.

Table 2. Displacement patterns for DDBD of bridges

BRIDGE	BALANCED MASS AND STIFFNESS	NO BALANCED MASS AND STIFFNEES
FRAME	RBT or EMS	EMS
WEAK ABUTMENTS	RBT or EMS	EMS
STRONG ABUTMENTS	FMS or EMS	FMS
ONE EXPANSION JOINT	LDP1 or EMS	EMS
TWO EXPANSION JOINTS	LDP2 or EMS	EMS
MORE THAN TWO EXPANSION JOINTS	EMS	EMS
		

A detailed explanation of all the steps involved in the application of DDBD is presented next.

3.1 Design Objective

In DDBD, a design objective or performance objective is defined by specification of the seismic hazard and the design limit state to be met under the specified seismic hazard. The seismic hazard is represented by an elastic displacement design spectrum (Fig 3). The

design spectrum is characterized by a Peak Spectral Displacement, PSD , and a corner period, T_c . The design limit state can be based on material strain limits, ductility, drift or any other damage or stability index. DDBD allows any combination of seismic hazard and design limit state; therefore, it can be used as a tool for Performance Based Seismic Engineering. Some of the most common design limit states are:

Life safety

This limit is used in the AASHTO Guide Specifications for LRFD Seismic Bridge Design (Imbsen, 2007) for bridges in Seismic Design Category (SDC) “D”. It is intended to protect human life during and after a rare earthquake. This limit implies that the bridge has low probability of collapse but may suffer significant damage in piers and partial or complete replacement may be required. To compute pier displacements to meet the life safety limit the ductility limits proposed in the AASHTO LRFD Guides (Imbsen, 2007) can be used. For single column bents ductility equals five. For multiple column bents, ductility equals six. For pier walls in the weak direction, ductility equals five. For pier walls in the strong direction, ductility equals one.

Damage control.

This limit is more restrictive than the life safety limit state. It sets the limit, beyond which damage in piers is not longer economically repairable due to failure of the transverse reinforcement (Kowalsky, 2000). For circular reinforced concrete columns typical strains related to this limit state are 0.018 for concrete in compression and 0.06 for steel in tension.

Specific values of compression strain for the confined concrete can be estimated using the energy balance approach developed by Mander (1988). In this model (Eq. 7), the damage-control concrete strain, $\varepsilon_{c,dc}$, is a function of volumetric transverse steel ratio, ρ_v , yield stress of the transverse steel reinforcement, f_{yh} , ultimate strain of the transverse steel reinforcement, ε_{su} , compressive strength of the confined concrete, f'_{cc} (Eq. 8) compressive strength of the unconfined concrete, f'_c , and the confinement stress f_l (Eq. 9).

$$\varepsilon_{c,dc} = 0.004 + 1.4 \frac{\rho_v f_{yh} \varepsilon_{su}}{f'_{cc}} \quad (\text{Eq. 7})$$

$$f'_{cc} = f'_c \left(2.254 \sqrt{1 + \frac{7.94 f_1}{f'_c}} - 2 \frac{f_1}{f'_c} - 1.254 \right) \quad (\text{Eq. 8})$$

$$f_1 = 0.5 \rho_v f_{yh} \quad (\text{Eq. 9})$$

The damage control displacement for single column or multiple column bents can then be computed based on the damage control strains using the plastic hinge method (Priestley and Calvi, 1993). This method is covered in Section 3.2.4.

Serviceability

This limit is more restrictive than the damage control limit state. It sets the limit beyond which damage in piers needs repair (Kowalsky, 2000). For circular reinforced concrete columns, typical strains related to this limit state are 0.004 for concrete in compression and 0.015 for steel in tension. The steel tension strain is defined as the strain at which residual cracks widths would exceed 1 mm. Serviceability pier displacement can be computed with the plastic hinge method covered in Section 3.2.4.

Stability limit

In addition to damage-based limit states, a stability criterion must also be specified as part of the design objective. According to the AASHTO guide specification (Imbsen, 2007), P-Δ effects can be neglected in the design of piers when the stability index is less than 25%. For application in DDBD, Priestley et al (2007) suggest that if the stability index is higher than 8%, P-Δ effects should be counteracted by an increase in the strength of the pier. However, stability index should not exceed 30%.

3.2 Determination of target displacement

Perhaps the most important step of the DDBD procedure is to determine the target displacement profiles in the transverse and longitudinal directions of the bridge. This process is executed in two steps: (1) Target displacements are computed for all earthquake resisting elements; (2) Target profiles for transverse and longitudinal response are proposed so that one or more elements meet their target displacements. No element must exceed its target displacement. The proposed target profiles must be consistent with the expected dynamic response of the bridge. Therefore in most cases, it will not be possible that all elements meet their target displacements and there will be one or two elements controlling the displacement profiles of the bridge. A detailed explanation on how to determine the target displacements for superstructures, abutments and piers, and the target displacement profiles for a bridge is presented next.

3.2.1 Plan Curvature

This feature cannot be explicitly accounted for in DDBD. Plan curvature complicates the definition of two principal design axes, and makes it difficult to apply of DDBD, since the method requires the determination of target displacement profiles in each principal direction independently.

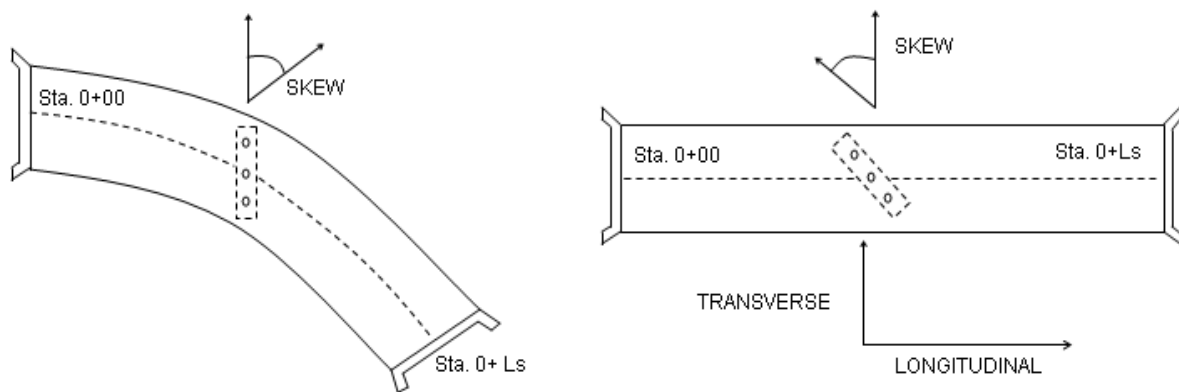


Figure 7. Curve bridge unwrapped to be designed as straight

A practical solution suggest that bridges with subtended angles of 90 degrees or less can be unwrapped and designed as straight bridges (Fig. 7). This is currently recommended in other bridge design codes (Caltrans, 2004; Ibsen 2007). Span lengths and skew angles in the equivalent straight bridge must be the same as in the curved bridge. Gravity induced forces, especially those resulting from the curved geometry, must be carefully considered and combined with seismic actions. (see Section 3.8.1).

3.2.2 Superstructure target displacement

It is a common strategy to design bridges in which damage and energy dissipation take place in the piers and abutments while the superstructure is protected and designed to remain elastic. The reason is that the substructure elements can be effectively designed to be ductile and dissipate energy while most superstructures cannot.

Current displacement-based practice (Ibsen, 2007; Caltrans, 2004) focuses on a displacement demand-capacity check for piers and ignores the limited displacement capacity of the superstructure. The implication of this is that while piers can have enough displacement capacity to cope with seismic demand, the superstructure might not. Therefore, a design based purely on pier displacement capacity could lead to bridges in which the superstructure suffers unaccounted damage.

If a target displacement is determined for the superstructure, this should meet the serviceability or other more restrictive strain limits or should be controlled by the displacement capacity of expansion joints. This discussion applies only to DDBD of bridges in the transverse direction. Bridge superstructures are usually stiff and strong in their axis, so their performance is not an issue when designing in the longitudinal direction.

Determining a superstructure target displacement is important for design of bridges responding with a flexible transverse displacement pattern, including: bridges with strong abutments, bridges with weak and flexible superstructures, bridges with unbalanced mass and stiffness.

The DDBD framework allows easy inclusion of superstructure transverse target displacement into the design procedure. The transverse target displacement profile of the bridge must be defined accounting for the target displacement of the piers, abutments and target displacement of the superstructure.

The determination of a target displacement for the superstructure requires moment curvature analysis of the superstructure section and double integration of the curvature profile along the length of the superstructure. Moment curvature analysis should account for expected material properties and strains caused by gravity loads. The result of the moment curvature analysis is the target curvature to meet the specified strain limits. Other important result is the flexural stiffness of the superstructure, which is also needed in design.

If it is believed that the target displacement of the superstructure should be controlled by yielding of the longitudinal reinforcement of a concrete deck, a yield curvature as target curvature can be estimated with Eq. 10. Where w_s is the width of the concrete deck and ε_y is the yield strain of the steel reinforcement. The yield curvature of a section is mainly dependent on its geometry and it is insensitive to its strength and stiffness (Priestley, 2007).

$$\phi_{ys} = \frac{2\varepsilon_y}{w_s} \quad (\text{Eq. 10})$$

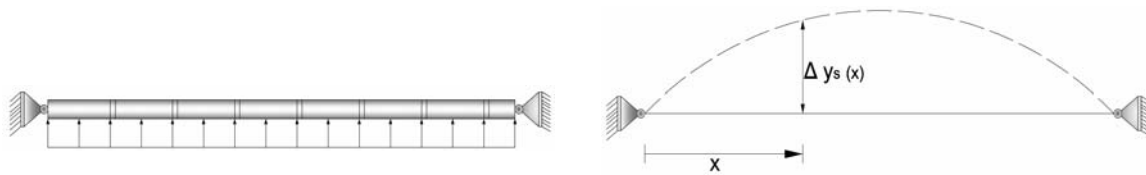


Figure 8 - Assumed superstructure displacement pattern

Assuming that the superstructure responds in the transverse direction as a simply supported beam, with the seismic force acting as a uniform load (Fig. 8), the curvature along the superstructure, $\phi_{s(x)}$, as a function of the target curvature of the superstructure, ϕ_{sT} , is given by Eq. 11. Double integration of the curvature function results in the target

displacement function shown as Eq. 12. Where L_s is the length of the superstructure and x is the location of the point of interest.

$$\phi_{s(x)} = \frac{4\phi_{ys}x}{L_s} - \frac{4\phi_{ys}x^2}{L_s^2} \quad (\text{Eq. 11})$$

$$\Delta_{Ts} = \phi_{Ts} \left[\frac{2x^4 - 4L_s x^3 + 2L_s^3 x}{6L_s^2} \right] \quad (\text{Eq. 12})$$

Eq. 12 gives the target displacement relative to the abutments. However, since the abutments are also likely to displace, Eq. 13 should be added to Eq. 12 to obtain a total target displacement. In Eq. 13, Δ_1 and Δ_n are the displacements of the initial and end abutment respectively.

$$\Delta_A = \Delta_1 + \frac{\Delta_n - \Delta_1}{L_s} x \quad (\text{Eq. 13})$$

$$\Delta_{Tsi} = \phi_{Ts} \left[\frac{2x_i^4 - 4L_s x_i^3 + 2L_s^3 x_i}{6L_s^2} \right] + \Delta_1 + \frac{\Delta_n - \Delta_1}{L_s} x_i \quad (\text{Eq. 14})$$

In Eq. 14, x is replaced by the location of each pier, x_i , to get the target displacement of the superstructure Δ_{Tsi} at that specific point. If Δ_{Tsi} is less than the target displacement of the pier, then Δ_{Tsi} controls design and becomes the design target displacement for the pier. An example that illustrates the application of this model is presented in Section 5.1

3.2.3 Abutment target displacement

Due to specific configurations and design details, an appropriate estimation of lateral target displacement will in most cases require a nonlinear static analysis of the abutment that has been previously designed for non-seismic loads. Instead of such analysis, a gross estimation of the displacement that will fully develop the strength of the fill behind the back or wing walls can be obtained with Eq. 15 (Imbsen, 2008). In this equation, f_h is a factor taken as 0.01 to 0.05 for soils ranging from dense sand to compacted clays and H_w is

the height of the wall. This relation might be useful in the assessment of a target displacement for integral abutments or seat-type abutments with knock-off walls.

$$\Delta_T = f_h H_w \quad (\text{Eq. 15})$$

3.2.4 Pier target displacement

Any type of bridge pier can be designed with DDBD as long as: (a) a target displacement can be easily estimated prior design; b) a relation between displacement and equivalent damping can be established. The first requirement is usually easy to comply knowing that the relation between strain in the plastic hinge region and displacement at the top of a pier is independent from the strength and stiffness of the pier.

The second item requires an assessment of design ductility and the use of an existing ductility-damping model such as those presented in Section 2.1. The determination of ductility demand requires knowledge of yield displacement which is calculated as part of the target displacement determination. As a result of this, the design of most common types of piers used in highway bridges can be easily implemented in DDBD. This includes piers with isolation/dissipation devices and piers with soil-structure interaction.

Table 3 - Parameters for DDBD of common types of piers

PIER TYPE	Effective Height H_p		Yield Disp. Factor α		Shear Height H_s	
	Transv.	Long.	Transv.	Long.	Transv.	Long.
Single column integral bent	$H+H_{sup}+L_{sp}$	$H+2L_{sp}$	1/3	1/6	H_p	$H_p/2$
Single extended drilled shaft integrall bent	L_e+H_{sup}	L_e+L_{sp}	varies	varies	H_p	$H_p/2$
Single column non-integral bent pinned in long direction	$H+H_{sup}+L_{sp}$	$H+L_{sp}$	1/3	1/3	H_p	H_p
Single extended-drilled-shaft non-integral bent pinned in long direction	L_e+H_{sup}	L_e	varies	varies	H_p	$H_p/2$
Multi column integral bent	$H+2L_{sp}$	$H+2L_{sp}$	1/6	1/6	$H_p/2$	$H_p/2$
Multi extended-drilled-shaft integrall bent	L_e+L_{sp}	L_e+L_{sp}	varies	varies	$H_p/2$	$H_p/2$
Multi column integral bent with pinned base	$H+L_{sp}$	$H+L_{sp}$	1/3	1/3	H_p	H_p
Multi column bent pinned in longitudinal direction	$H+2L_{sp}^*$	$H+L_{sp}^*$	$1/6^*$	$1/3^*$	$H_p/2^*$	H_p^*
Multi extended-drilled-shaft non-integral bent pinned in long direction	L_e^*	L_e^*	varies [*]	varies [*]	$H_p/2^*$	H_p^*

* These are in-plane and out-of-plane values and must be corrected for skew to get transverse and longitudinal values

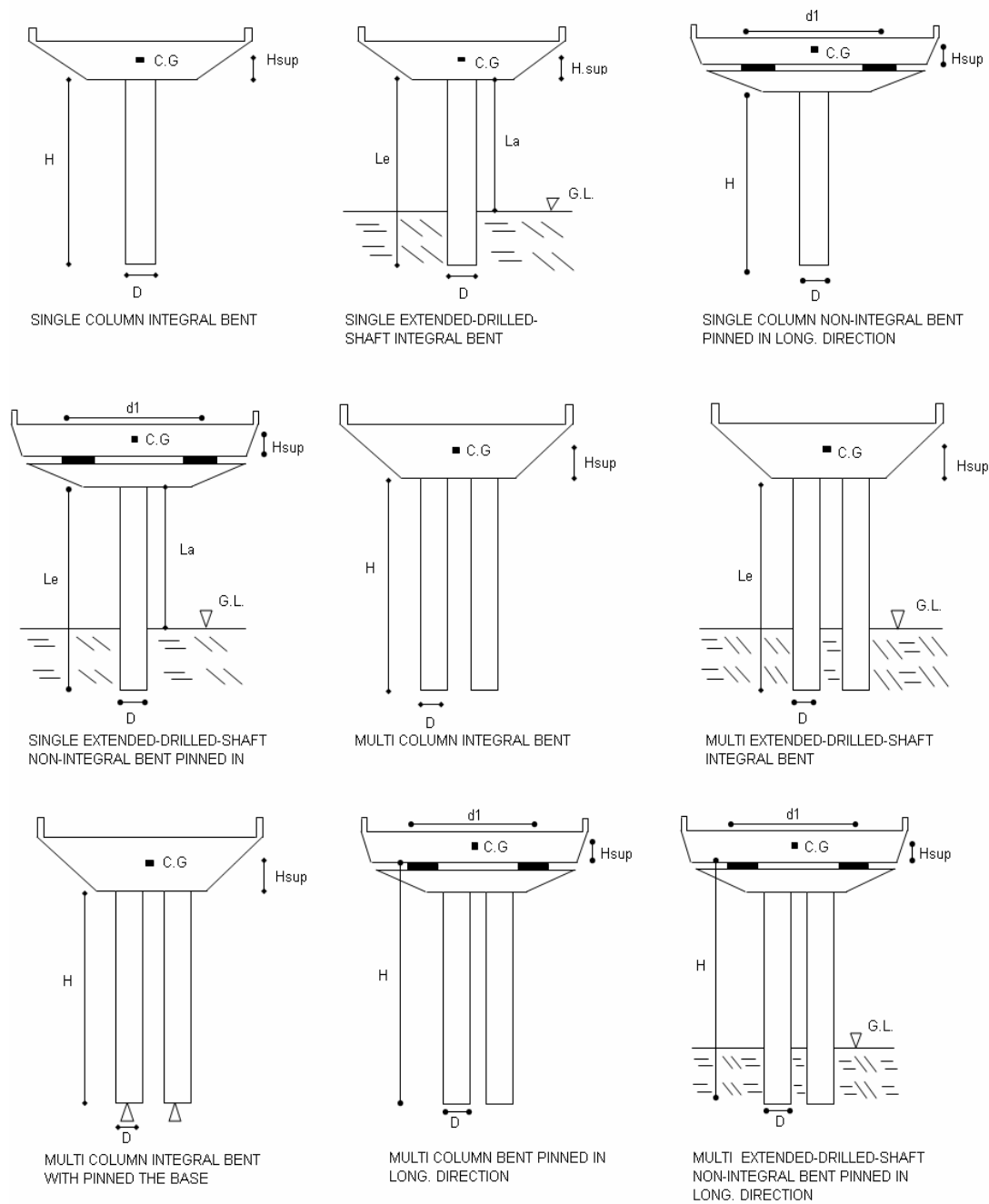


Figure 9 - Common types of piers in highway bridges

A graphic description of common types of reinforced concrete piers used in conventional bridges is presented in Fig. 9. In relation to that figure, Table 3 shows values for: the effective height of the pier H_p , yield displacement factor α , and shear height H_s .

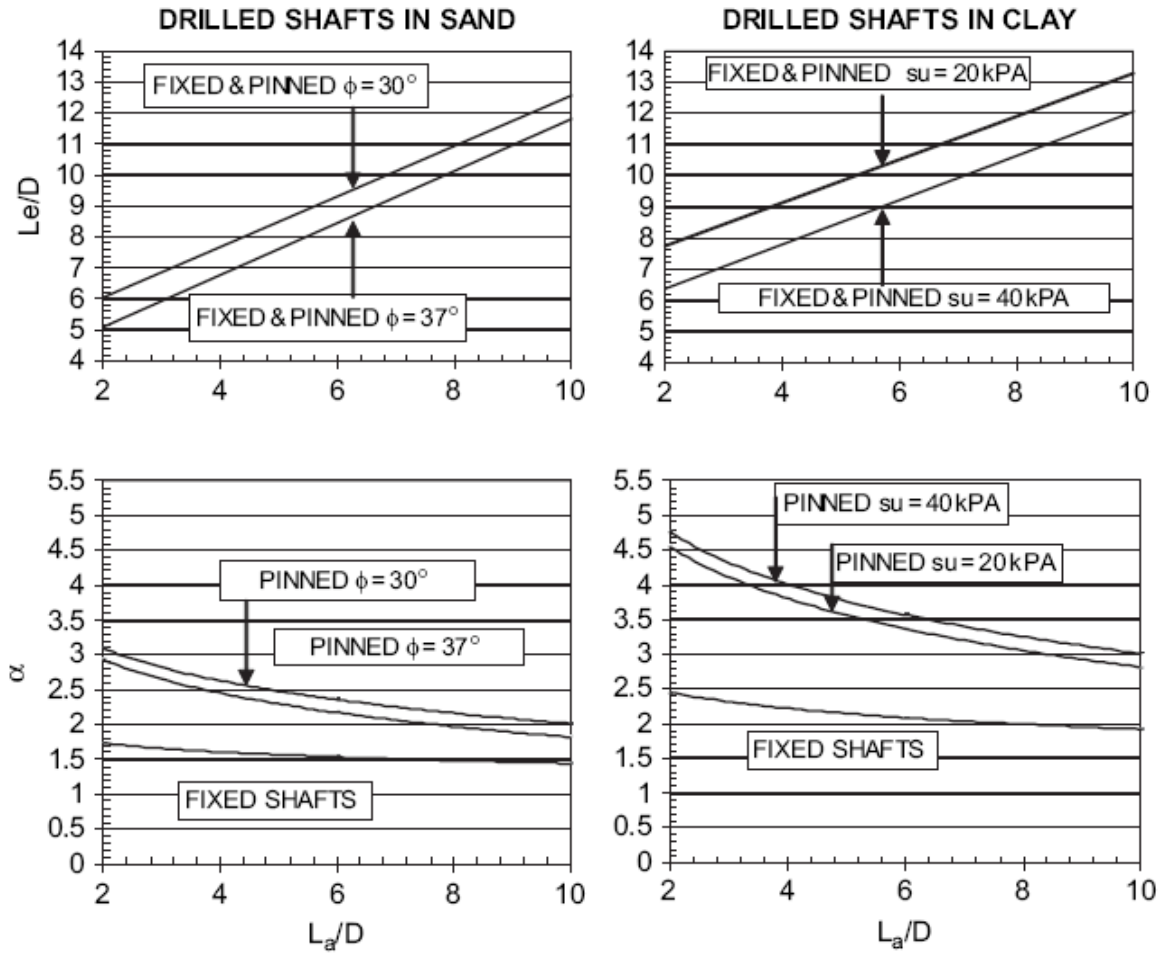


Figure 10 - L_e and α for definition of the equivalent model for drilled shaft bents (Suarez and Kowalsky, 2007)

These parameters are given for design in transverse and longitudinal axes of the bridge. In Table 3, H is the height of column, L_e is the effective height of drilled shaft, H_{sup} is the height from the soffit to the centroid of the superstructure and L_{sp} is the strain penetration length. The parameters L_e and α for drilled shaft bents are shown in Fig. 10 in terms of the type of soil, above ground height of the bent, L_a , and diameter of the drilled shaft section D .

Plastic Hinge Method

Strain-based target displacements are determined using the plastic hinge method (Priestley et al, 2007). For any type of pier listed in Table 3, the target displacement, Δ_t , along the

transverse and longitudinal axis of the bridge is estimated with Eq. 16. In this equation, Δ_y is the yield displacement of the pier, ϕ_t and ϕ_y are the target and yield curvature respectively, L_p is the plastic hinge length and H_p is the effective height of the pier defined in Table 3.

$$\Delta_T = \Delta_y + (\phi_t - \phi_y)L_p H_p \quad (\text{Eq. 16})$$

The target curvature is determined in terms of the target concrete strain, $\epsilon_{c,T}$, target steel strain, $\epsilon_{s,T}$, and neutral axis depth, c , with Eq. 17. The target curvature can be controlled by the concrete reaching its target strain in compression or the flexural reinforcement reaching its target strain in tension.

$$\phi_{dc} = \min \left[\frac{\epsilon_{c,T}}{c}, \frac{\epsilon_{s,T}}{D - c} \right] \quad (\text{Eq. 17})$$

The neutral axis depth can be estimated with Eq. 18, where P is the axial load acting on the element and A_g is the gross area of the section (Priestley et al, 2007)

$$c = 0.2D \left(1 + 3.25 \frac{P}{f'_{ce} A_g} \right) \quad (\text{Eq. 18})$$

The yield curvature ϕ_y is independent of the strength of the section and can be determined in terms of the yield strain of the flexural reinforcement ϵ_y and the diameter of the section D with in Eq. 19 (Priestley et al, 2007)

$$\phi_y = 2.25 \frac{\epsilon_y}{D} \quad (\text{Eq. 19})$$

The yield displacement Δ_y is given by Eq. 20, where α is given in Table 3 for transverse and longitudinal directions. For extended drilled shaft bents, α is shown in Figure 10.

$$\Delta_y = \alpha \phi_y (H_p)^2 \quad (\text{Eq. 20})$$

Life safety target displacement

Is computed introducing the ductility limits given in Section 3.1 in Eq. 21.

$$\Delta_T = \Delta_y \mu \quad (\text{Eq. 21})$$

Damage control target displacement

The damage control concrete compression strain $\varepsilon_{c,dc}$ must be first computed with Eq. 7. The damage control tension strain for the flexural reinforcement is $\varepsilon_{s,dc} = 0.06$ (Kowalsky, 2000) (See Section 3.1). These values are used in Eq. 17 to find ϕ_t and finally Eq. 16 is used to get the target displacement.

Serviceability target displacement

The strain limits in Section 3.1 are used to compute a target curvature and then a target displacement with Eq. 16

Target displacements for SDC “B” and “C”

For these SDCs, the equations given in AASHTO (Ibsen, 2007) for the assessment of displacement capacity for moderate plastic action (Eq. 23) and minimal plastic action (Eq. 24) can also be used in DDBD to get a target displacement. In Eq. 23 and Eq. 24, H_c is the clear height of the columns and Λ is 1 for columns in single bending and 2 for columns in double bending.

$$\Delta_c = 0.003H_c \left(-2.32 \ln \left(\frac{D}{H_c} \Lambda \right) - 1.22 \right) \geq 0.003H_c \quad (\text{m}) \quad (\text{Eq. 23})$$

$$\Delta_c = 0.003H_c \left(-1.27 \ln \left(\frac{D}{H_c} \Lambda \right) - 0.32 \right) \geq 0.003H_c \quad (\text{m}) \quad (\text{Eq. 24})$$

Stability-based target displacement

A target displacement for a bridge pier to meet a predefined value of the stability index, θ_s , can be estimated with Eq. 25 (Suarez and Kowalsky 2008b), where the parameters a , b , c and d are given in Tables 4 and 5 for piers on rigid foundations and extended drilled shaft bents in different types of soils. Table 4 gives the parameters for near fault sites and Table 5 for far fault sites. The parameter C in Eq. 25 is computed with Eq. 26 in terms of the peak spectral displacement, PSD , the corner period, T_c , the axial load acting on the pier, P , the effective mass on the pier, M_{eff} , and the height of the pier H .

$$\mu_{\theta_s} = a + bC + c \frac{C - d}{C} \quad (\text{Eq. 25})$$

$$C = \frac{T_c \Delta_y}{2\pi PSD} \sqrt{\frac{P}{\theta_s M_{eff} H}} \quad (\text{Eq. 26})$$

If a bridge pier is designed as a stand-alone structure, M_{eff} can be computed taking a tributary area of superstructure and adding the mass of the cap-beam and a portion of the mass of the pier itself (1/3 is appropriate). If the target displacement is being determined for a pier that is part of a continuous bridge, M_{eff} is computed with Eq. 27 as a fraction of the effective mass of the bridge, M_{EFF} . The effective mass of the bridge is computed as with Eq. 2 and v_i is computed with Eq.31

$$M_{eff} = v_i M_{EFF} \quad (\text{Eq. 27})$$

Table 4 - Parameters to define Eq.15 for far fault sites

	Rigid Base	Clay-20 Pinned	Clay-20 Fixed	Clay-40 Pinned	Clay-40 Fixed	Sand-30 Pinned	Sand-30 Fixed	Sand-37 Pinned	Sand-37 Fixed
a	1.256	0.839	0.885	0.961	0.909	1.010	1.468	1.105	1.053
b	-0.127	-0.021	-0.034	-0.042	-0.043	-0.047	-0.078	-0.055	-0.061
c	-0.766	-0.657	-0.693	-0.737	-0.697	-0.774	-1.160	-0.847	-0.792
d	0.731	0.724	0.860	0.644	0.877	0.677	0.546	0.620	0.852

Table 5 - Parameters to define Eq.15 for near fault sites

	Rigid Base	Clay-20 Pinned	Clay-20 Fixed	Clay-40 Pinned	Clay-40 Fixed	Sand-30 Pinned	Sand-30 Fixed	Sand-37 Pinned	Sand-37 Fixed
a	1.146	0.803	0.924	0.868	0.912	0.963	1.210	0.966	1.053
b	-0.112	0.000	-0.013	-0.015	-0.023	-0.028	-0.035	-0.019	-0.061
c	-0.799	-0.728	-0.833	-0.754	-0.793	-0.814	-1.058	-0.850	-0.792
d	0.917	0.965	0.939	0.920	0.980	0.869	0.759	0.869	0.852

The target ductility obtained from Eq. 25 is multiplied to the yield displacement of the pier to get the stability-based target displacement. The target ductility obtained from Eq. 25 is plotted in Figs 11 and 12 for a range of values of C . In both figures it is observed that ductility is very sensitive to changes in C when C is less than 0.5. The differences in ductility for the different models come from the differences in equivalent damping (see Section 2.1). If two piers have the same value of C , the one with more damping develops less ductility to reach the stability limit. The reason is that the pier with less damping requires more strength. The different damping models have less effect in the relation between μ_{0s} and C for near fault sites.

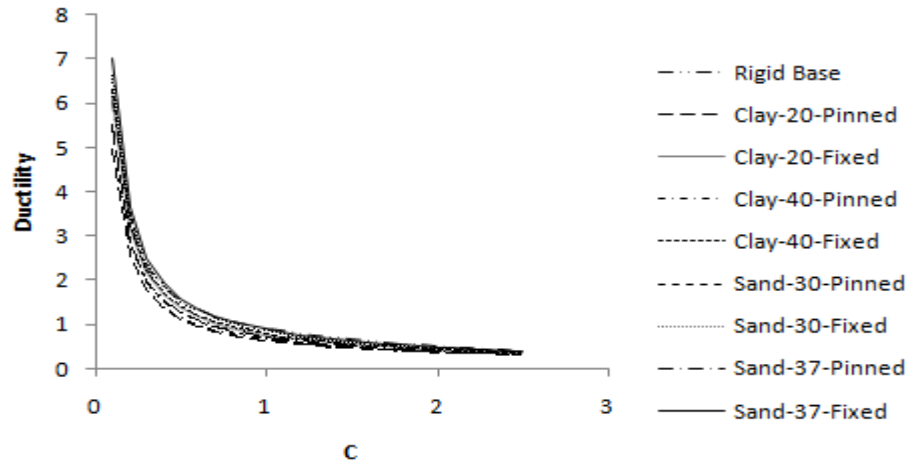


Figure 11. Ductility vs. C for far fault sites

The use of Eq. 25 avoids the need of iteration in DDBD for designs controlled by P - Δ effects. The proposed model is accurate for design of piers as stand-alone structures or in the case of regular bridges with a balanced distribution of mass and stiffness. If the model is used with irregular bridges, it will produce conservative estimates of target displacement

(Suarez and Kowalsky, 2008b). An example that illustrates the application of this model is presented in Section 5.2

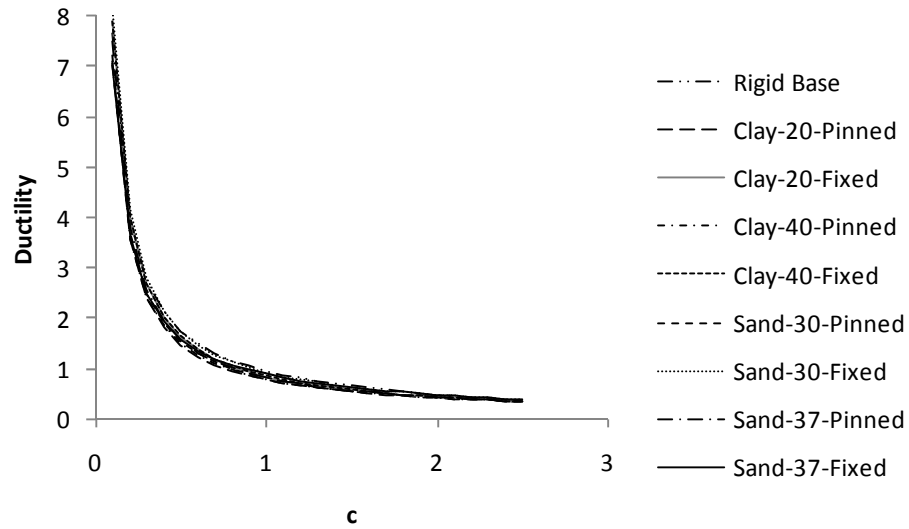


Figure 12. Ductility vs. C for near fault sites

3.3 Skewed piers or abutments

From a design perspective, the effect of a skewed configuration is that in-plane and out-of-plane response parameters of abutments and piers are no longer oriented in the principal design directions of the bridge (Fig. 12).

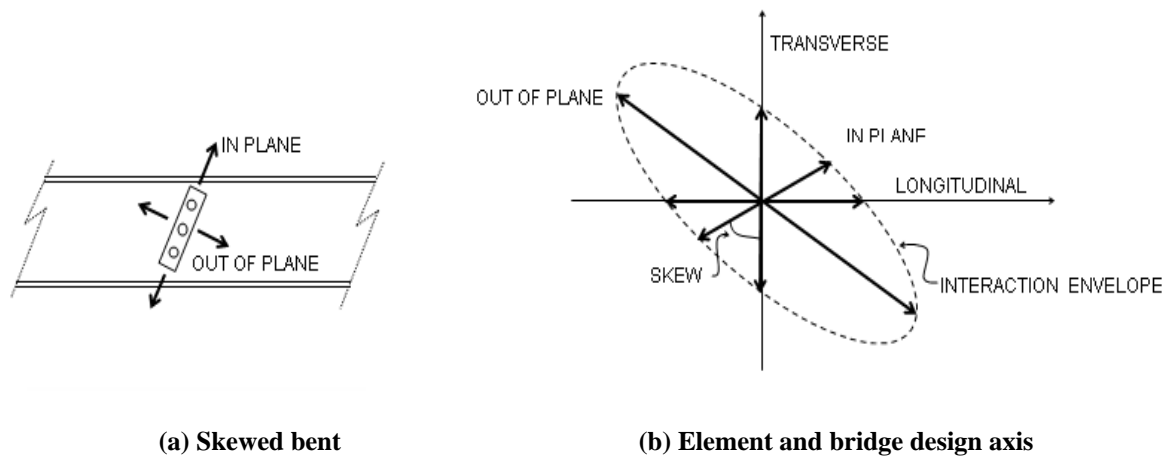


Figure 12 - Design axes in skewed elements

The effects of skew can be considered in DDBD by determining the projection of any response parameter such as yield displacement Δ_y , target displacement Δ_T , shear height H_s and others, with respect to the transverse and longitudinal direction of the bridge. Such determination can be done using an elliptical interaction function between the in-plane and out-of-plane response, as given by the following equations:

$$rp_T = rp_{IN} + skew \frac{rp_{OUT} - rp_{IN}}{90} \quad (\text{Eq. 28})$$

$$rp_L = rp_{OUT} + skew \frac{rp_{IN} - rp_{OUT}}{90} \quad (\text{Eq. 29})$$

Where, rp_{IN} is the value of the response parameter in the in-plane direction of the element, rp_{OUT} is the response parameter in the out-of-plane direction of the element, rp_T is the projection of the response parameter in the transverse direction of the bridge and rp_L is the projection of the response parameter in the longitudinal direction of the bridge. An example that illustrates the application of this model is presented in Section 5.3.

3.4 Determination of target displacement profiles

Once the target displacement has been determined for the superstructure, abutments and piers, considering skew if necessary, the next step is to propose a target displacement profile along the transverse and longitudinal directions of the bridge.

3.4.1 Transverse displacement profiles

As was mentioned before, much of the effort in the application of DDBD for transverse design of bridges is in the selection or determination of the target displacement profile. Previous research conducted by Dwairi and Kowalsky (2006) focused on the identification of displacement patterns for symmetric and asymmetric bridge configurations using Inelastic Time History Analysis (ITHA). Three types of displacement patterns were identified, namely: Rigid Body Translation (RBT), Rigid Body Translation with Rotation (RBTR) and flexible pattern. These patterns were found to be highly dependent on the

superstructure to substructure stiffness ratio, bridge regularity and type of abutment. It was also found that only symmetrical regular bridges with stiff superstructures and free abutments respond with a RBT pattern.

Recent research (Suarez and Kowalsky, 2008) has shown that bridges frames and bridges with weak abutments that comply with balanced mass and stiffness requirements of the AASHTO guide specification (Imbsen, 2007) can be designed in the transverse direction assuming a rigid body translation pattern. The Balanced Mass and Stiffness (BMS) index is computed with Eq. 30, where m_i and m_j are the lumped mass at piers i and j and K_{pi} and K_{pj} are the stiffness of piers i and j . This index is computed in two ways, BMS1 is the least value that results of all combinations of any two piers and BMS2 is the least value that results from all combinations of adjacent piers. If $BMS1 > 0.50$ and $BMS2 > 0.75$ the bridge is considered regular.

$$BMS = \frac{M_i K_{pj}}{M_j K_{pi}} \quad (\text{Eq. 30})$$

AASHTO (Imbsen, 2007) and Caltrans (1996) recommend bridges to comply with the balanced mass and stiffness requirements described above. This is to avoid torsion and uneven distribution of damage in the structures. Therefore, it is likely that most conventional highway bridges can be designed with DDBD using a rigid body displacement pattern. In such a case, it is expected that the transverse displacement of all piers be the same and thereof, the amplitude of displacement profile is controlled by the pier or abutment with the least target displacement (See Table 2). When a rigid body displacement pattern is used, the application of DDBD is direct as shown in Fig. 6 This process is cover in detail in Section 3.5.1.

In the case of bridges with integral abutments or other types of strong abutments, designed to limit the displacement of the superstructure, the transverse displacement pattern is flexible and its shape depends mainly on the relation between the stiffness of the superstructure, abutments and piers (See Table 2). Since the stiffness of the piers and abutments depends on their strength, which is not know at the beginning of the process, the shape of the displacement pattern of this type of bridges must be assumed and refined

iteratively. This is done using the First Mode Shape (FMS) or the Effective Mode Shape (EMS) algorithms shown in Fig. 6 and described in detail in Sections 3.5.2 and 3.5.3. The amplitude of the displacement profiles is set so that no element exceeds their target displacement.

For bridges with up to two internal expansion joints in the superstructure, research by the authors (Suarez and Kowalsky, 2008a) indicated that predefined linear displacement patterns can be used to execute DDBD directly. Such displacement patterns are shown in Table 2 and Fig. 13, the amplitude of the displacement profiles is set so that no element exceeds their target displacement.

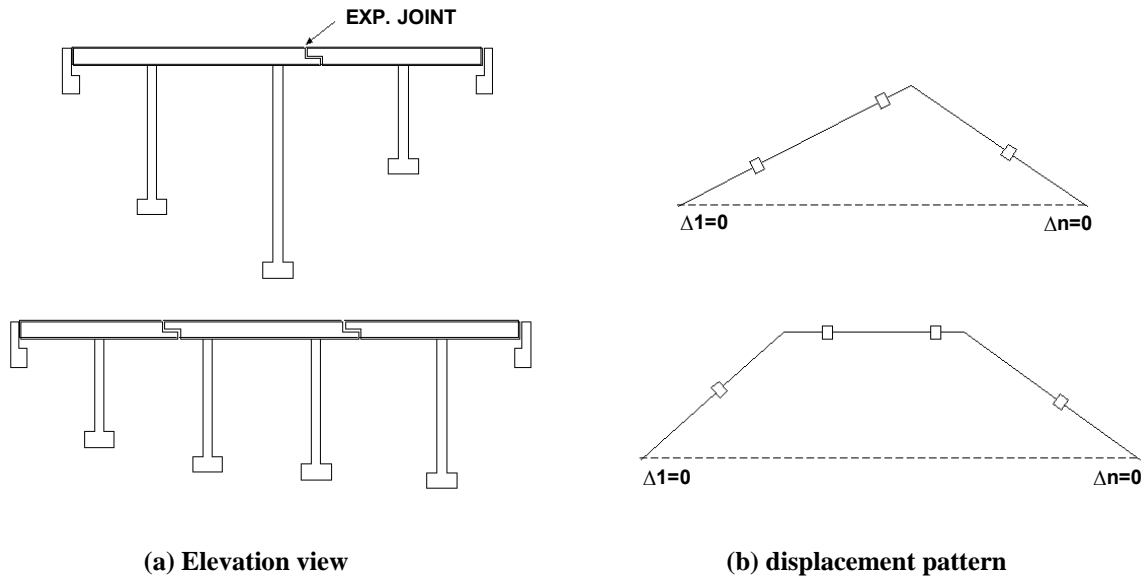


Figure 13 - Displacement patterns for bridges with expansion joints

3.4.2 Longitudinal displacement profiles

Continuous superstructures are usually strong and axially rigid, therefore it is reasonable to assume that the superstructure displaces longitudinally as a rigid body, constraining the displacements of all piers to be the same. In this case, the amplitude of the displacement profile is controlled by the pier or abutment with the least target displacement and DDBD is applied directly as shown in Fig. 6.

For superstructures with expansion joints, two possible displacement patterns must be considered (Fig. 14), one with the expansion joint gaps closing towards one end of the bridge and the other with the joints closing towards the opposite end of the bridge. These two alternative patterns are likely to result in different generalized displacement for the bridge (See Section 2, Eq. 1). The least generalized displacement controls design.

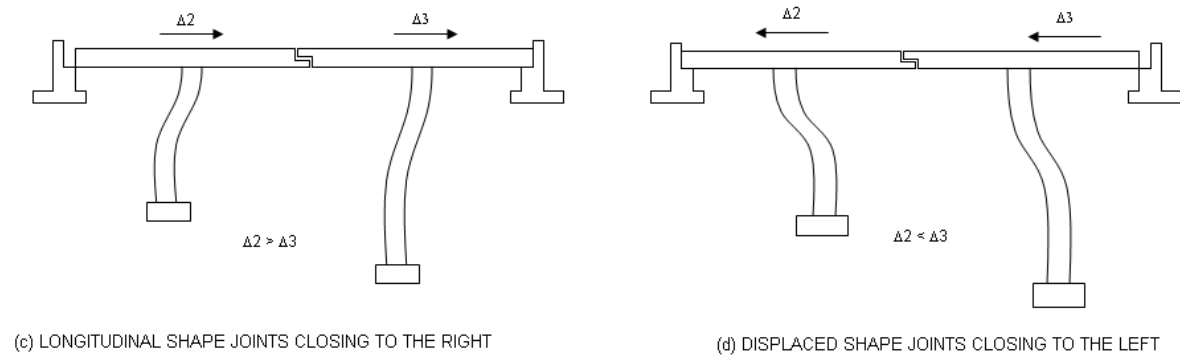


Figure 14 – Longitudinal displacement pattern for bridges with expansion joints

3.5 DDBD IN THE TRANSVERSE DIRECTION

DDBD is applied in the transverse direction as part of the overall procedure showed in Fig. 5. A summary of the steps involved in the transverse design is presented in Fig. 6. In this figure it is shown that there are three different design algorithms. A detailed description of the general steps and algorithms is presented next.

Strength Distribution

If a bridge is designed to suffer damage during the design earthquake, it is possible that most of its piers and abutments (if present) develop their nominal strength and behave inelastically. Therefore, the distribution of strength among bents and abutments is not longer a unique matter of initial stiffness but a designer's choice constrained by equilibrium.

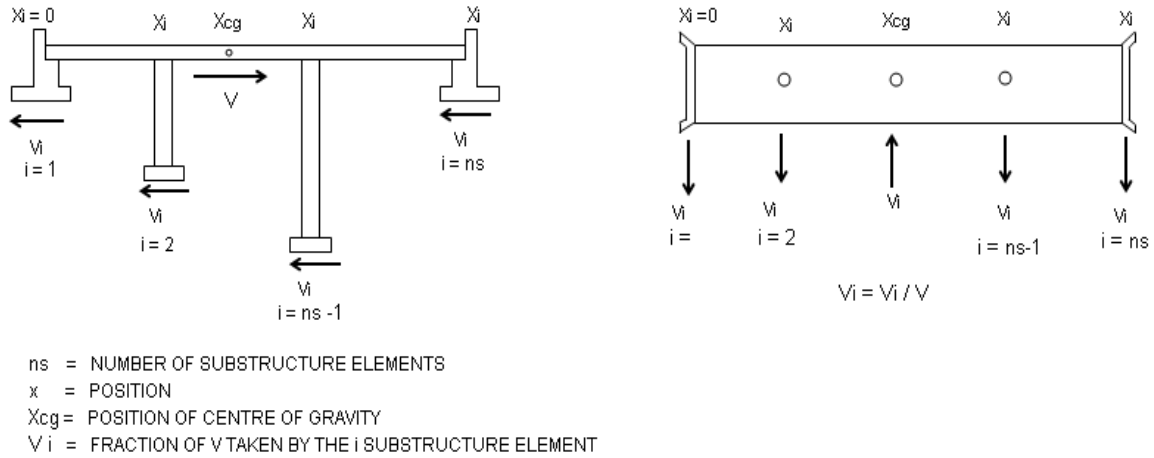


Figure 15 – Strength distribution in the longitudinal and transverse directions

In most bridges, there are two load paths for the inertial forces developed during an earthquake, one is from the superstructure through the abutments and the other is from the superstructure through the piers to the foundation soil (Fig. 15). The ratio of total base shear V taken by the superstructure to the abutments v_s is generally unknown and must be assumed at the beginning of the design process. The ratio of base shear taken by the piers, $v_p = 1 - v_s$, must be distributed among them satisfying equilibrium. Some of the possible distributions of strength are:

- A distribution to obtain pier columns with the same flexural reinforcement ratio, which is practical and leads to construction savings.
- A distribution with equal shear demand in all piers, which is appropriate for bridges with seismic isolation, to use the same device in all piers

Strength Distribution for columns with same reinforcement ratio

Since reinforced concrete sections with the same reinforcing ratio show similar ratios of cracked to gross section stiffness, a distribution of strength to get the same reinforcement ratio in all columns of the bridge can be computed with Eq. 31. This equation gives the ratio of total strength, v_i , taken by bent i , with n_i columns of diameter D_i , shear height H_{s_i} and ductility μ_i , required to satisfy force equilibrium. Table 3 defines H_s for different types of piers.

$$v_i = (1 - v_s) \frac{\frac{n_i \mu_i D_i^3}{H_{si}}}{\sum \frac{n_i \mu_i D_i^3}{H_{si}}} \quad \mu_i \leq 1 \quad (\text{Eq. 31})$$

Strength Distribution for equal shear in bents

Strength among piers can be distributed equally. This alternative is practical when designing bridges with isolation/dissipation devices on top of the bents. The reason is that the same device can be use in all bridge piers.

3.5.1 Direct procedure

This procedure applies to cases where a rigid body or other predefined displacement profile has been adopted for design (see Section 3).

Step1. Determine Target displacement profile

Follow Section 3.4

Step2. Determine properties of equivalent SDOF system

Using Eq. 1 and Eq. 2 the generalized displacement Δ_{sys} and the Effective mass M_{EFF} are found.

Step3. Compute ductility and equivalent damping

For each pier and abutment the ductility is computed as the ratio of the displacement in the target profile Δ_i and the yield displacement Δ_{yi} of the element. If the yield displacement Δ_y was not computed during the determination of target displacement, it should be computed with Eq. 20, with reference to Table 3.

Once ductility is known, the equivalent damping for each pier is computed with an appropriate model. See Section 2.1. For the abutments it is recommended to use equivalent damping values between 5% and 10%. The higher value of damping is appropriate when full soil mobilization is expected. Higher values of damping can be computed with Eq. 3 when plastic hinges are expected to develop in piles supporting the abutment at the target

displacement level. If elastic response is expected in the superstructure, damping between 2% and 5% should be used.

The equivalent damping computed for each element must be combined to obtain the equivalent damping for the substitute SDOF system. The combination is done in terms of the work done by each element (Kowalsky, 2002). The work done by the superstructure is computed with Eq. 32. The work done by each abutment is computed with Eq. 33 and Eq. 34. The work done by each pier is computed with Eq. 35. Finally the combined damping is computed with Eq. 36.

$$ws = \left[\Delta_{sys} - \frac{(\Delta_1 + \Delta_{nb})}{2} \right] v_s \quad (\text{Eq. 32})$$

$$wa_1 = \Delta_1 v_1 \quad (\text{Eq. 33})$$

$$wa_n = \Delta_n v_n \quad (\text{Eq. 34})$$

$$wp_i = \Delta_i v_i \quad (\text{Eq. 35})$$

$$\xi_{sys} = \frac{wa_1 \xi_1 + wa_n \xi_n + ws \xi_s + \sum_2^{n-1} wp_i \xi_i}{wa_1 + wa_n + ws + \sum_2^{n-1} wp_i} \quad (\text{Eq. 36})$$

Step 4. Determine the required strength

First the 5% damping elastic displacement spectrum is reduced to the level of damping of the structure (ξ_{sys}). To do this, a demand reduction factor is computed with Eq. 37 (Eurocode, 1998), where $\alpha = 0.25$ for near fault sites and $\alpha = 0.5$ for other sites. Then, the reduced displacement design spectra is entered with Δ_{sys} to find the required period, T_{eff} , for the structure. This is shown schematically in Fig. 3. This process has been synthesized in Eq. 38.

$$R_\xi = \left(\frac{7}{2 + \xi_{sys}} \right)^\alpha \quad (\text{Eq. 37})$$

$$T_{eff} = \frac{\Delta_{sys}}{PSD \cdot R_{\xi}} T_c \quad (\text{Eq. 38})$$

Based on the well know relation between stiffness, mass and period of a single degree of freedom system, the stiffness, K_{eff} , and then the strength, V , required for the equivalent system are obtained with Eq. 39 and Eq. 40 respectively.

$$K_{eff} = \frac{4\pi^2 M_{eff}}{T_{eff}^2} \quad (\text{Eq. 39})$$

$$V = K_{eff} \Delta_{sys} \quad (\text{Eq. 40})$$

Step 5. Distribute required strength

The required strength V_i is determined for each substructure element with Eq. 41. Finally, the design flexural strength, M_i , for the columns in each pier is computed according to the type of pier (Table 3) with Eq. 42.

$$V_i = v_i V \quad (\text{Eq. 41})$$

$$M_i = \frac{H_{st} V_i}{n_i} \quad (\text{Eq. 42})$$

3.5.2 First mode shape algorithm

This algorithm is applicable to cases where a flexible displacement pattern has been adopted and the response of the bridge is controlled by its first mode of vibration (See Table 3). This procedure is iterative and use elastic analysis of refine the assumed displacement pattern. This algorithm converges to the first mode inelastic shape of the structure.

Step1. Determine Target displacement profile

Follow Section 3.4

Step 2. Apply direct procedure

Conduct all the steps 2- 4 of the direct solution presented in Section 3.5.1

Step 3. Find a best estimate of the displacement pattern

Inertial forces consistent with the assumed displacement pattern are applied to a bridge model with stiffness secant to maximum response. This static analysis results in a displacement pattern that is a best approximation to the first mode shape of the bridge.

To perform the static analysis, a 2D model of the bridge is built (Fig. 16). In this model, the substructure elements are springs with secant stiffness computed with Eq.43. The superstructure is modeled as a series of frame elements. The loads apply to the model are the inertial forces, F_i , are computed with Eq. 44.

$$K_{effi} = \frac{V_i}{\Delta_i} \quad (\text{Eq. 43})$$

$$F_i = \frac{m_i \Delta_i}{\sum_1^n m_i \Delta_i} V \quad (\text{Eq. 44})$$

Once performed, the outcome of this analysis includes the displacements for each substructure element, Φ_i , and new estimates of the proportion of the total shear taken by the abutments, v_{r1} and v_{rn} . These values are computed with Eq. 45 and Eq. 46. If v_l and v_n where assumed at the beginning of the process, an error between the new and assumed values can be computed with Eq. 47 and Eq. 48.

$$v_{r1} = \frac{\Phi_1 K_1}{V} \quad (\text{Eq. 45})$$

$$v_{rn} = \frac{\Phi_n K_n}{V} \quad (\text{Eq. 46})$$

$$ERR_{v1} = abs\left(\frac{v_l - v_{r1}}{v_{r1}}\right) \quad (\text{Eq. 47})$$

$$ERR_{vn} = abs\left(\frac{v_n - v_{rn}}{v_{rn}}\right) \quad (\text{Eq. 48})$$

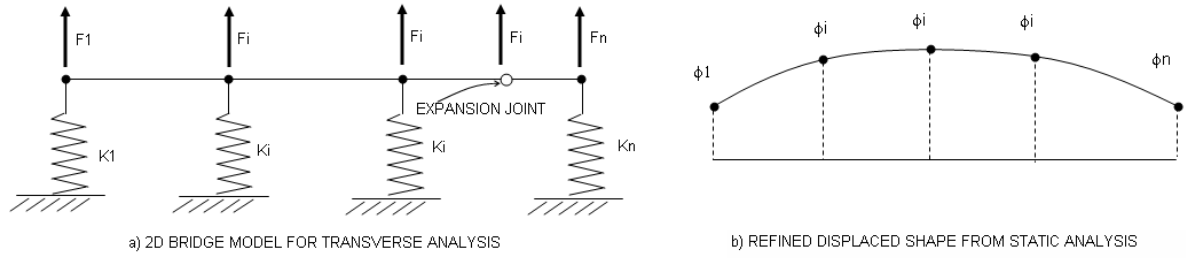


Figure 16 – 2D model of bridge with secant stiffness.

Step 4. Scaling the first mode shape to meet the design objective

This process must assure that no element in the bridge exceeds their previously calculated target displacement. This step is accomplished by calculating a scaling factor, Sf_i , for each element as shown in Eq. 49. Then, the least of the scaling factors is applied to the displacements computed in Step 3 to get a refined displacement profile (Eq. 50).

$$Sf_i = \frac{\Delta_{Ti}}{\Phi_i} \quad (\text{Eq. 49})$$

$$\Delta_{ri} = \Phi_i \min_{1}^n Sf_i \quad (\text{Eq. 50})$$

If the abutments are elastic, their target displacements must be enforced in the displaced shape, that is $\Delta_{r1} = \Delta_{y1}$ and $\Delta_{rn} = \Delta_{yn}$. An error between the previous displacement profile and the new displacement profile can be estimated with Eq. 51

$$ERR_{dp} = \sum_{i=1}^{i=n} (\Delta_{ri} - \Delta_i)^2 \quad (\text{Eq. 51})$$

Step 5. Check convergence and iterate

When applying this algorithm two assumptions are made: (1) The shape of the displacement pattern, (2) The proportion of total shear carried by the abutments (if present). If errors ER_{v1} and ER_{vn} and ER_{dp} are greater than a predefined tolerance, the procedure must be repeated from Step 2 the number of times required to get the errors

within the tolerance. In each iteration the proportion of base shear taken by the abutments and the displacement profile must be updated (i.e. $v_l = v_{rl}$, $v_n = v_{rn}$ and $\Delta_i = \Delta_{ri}$)

3.5.3 Effective mode shape algorithm

This algorithm is applicable to all cases (See Table 3), however due to its increased complexity, it is recommended to cases where a flexible displacement pattern is used and the response of the bridge is controlled by the combination of several modes of vibration.

This procedure is more complex and requires more effort than the First Mode Shape algorithm. However, this procedure captures the effects of higher modes of vibration in the displacement profile and in the element forces. This procedure is iterative and uses response spectrum analysis to refine the assumed displacement pattern. Its application follows the steps presented next:

Step1. Determine Target displacement profile

Follow Section 3.4

Step 2. Apply direct procedure

Conduct all the steps 2- 4 of the direct procedure presented in Section 3.5.1

Step 3. Find a best estimate of the displacement pattern

A response spectrum analysis is conducted with a model of the bridge in which the substructure elements have secant stiffness computed with Eq. 43. A composite acceleration response spectrum is used such as the one shown in Fig. 17. In the composite spectrum, the spectral ordinates corresponding to the effective period (T_{eff}) of the bridge are reduced by the factor R_ξ computed with Eq. 38 in Step 4 of the direct procedure. The spectral ordinates for periods shorter than T_{eff} are not reduced since the higher modes are likely to be elastic modes of response in the structure.

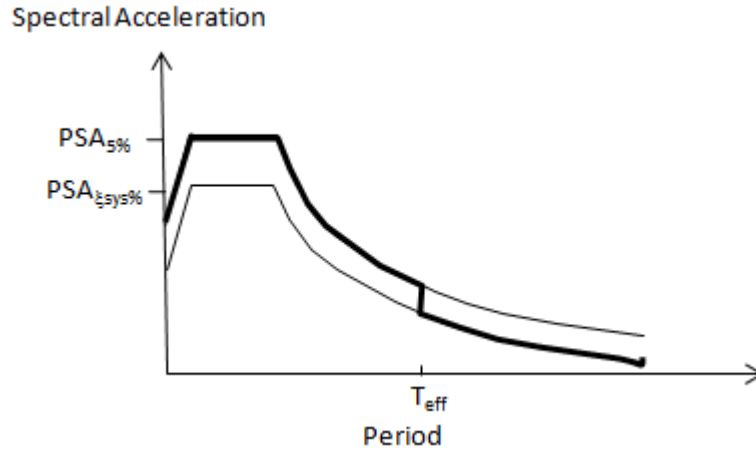


Figure 17 – Composite acceleration response spectrum

The outcome of this analysis includes the displacements for each substructure element, Φ_i , new estimates of the proportion of the total shear taken by the abutments, v_{r1} and v_m , and forces in the superstructure and abutments. Forces in inelastic piers are not considered since any demand in excess of the capacity of the piers is only a result of the elastic analysis. The proportion of shear taken by the abutments is computed with Eq. 45 and Eq. 46. If v_l and v_n were assumed at the beginning of the process, an error between the new and assumed values can be computed with Eq. 47 and Eq. 48.

Step 4. Scaling the first mode shape to meet the design objective

This process must assure that no element in the bridge exceeds their previously calculated target displacement. This step is accomplished by calculating a scaling factor, Sf_i , for each element as shown in Eq. 49. Then the least of the scaling factors is applied to the displacements computed in Step 3, to get a refined displacement profile (Eq. 50).

If the abutments are elastic, their target displacements must be enforced in the displaced shape, that is $\Delta_{r1} = \Delta_{y1}$ and $\Delta_{rn} = \Delta_{yn}$. An error between the previous displacement profile and the new displacement profile can be estimated with Eq. 51

Step 5. Check convergence and iterate

When applying this algorithm to two assumptions basic are made: (1) The shape of the displacement pattern, (2) The proportion of total shear carried by the abutments. If errors ER_{v1} and ER_{vn} and ER_{dp} are greater than a predefined tolerance, the procedure must be repeated from Step 2 the number of times required to get the errors within the tolerance. In each iteration the proportion of base shear taken by the abutments and the displacement profile must be updated (i.e. $v_l = v_{rl}$, $v_n = v_{rn}$ and $\Delta_i = \Delta_{ri}$)

3.6 DDBD in the longitudinal direction

Applying DDBD in the longitudinal direction of the bridge is generally simpler than doing it in the transverse direction. The steps involved are detailed next:

Step1. Determining target displacement profile

Due to high axial stiffness of the superstructure, a target displacement profile can be determined at the beginning of the process. There are two possibilities that must be considered:

- a) If there are not expansion joints in the superstructure nor at the abutments (if exist), all substructure elements are constrained to displace the same amount. Therefore, the substructure element with the least target displacement will control the target displacement of the bridge.
- b) If there are expansion joints in the bridge, two target displacement profiles must be considered, one with the bridge being pushed towards the end pier or abutment and the other with the bridge being pushed towards the initial pier or abutment (Fig. 14)

In any case then target profile must be scaled keeping in mind that no substructure element should exceed its target displacement.

Step 2. Computing system displacement and mass

The same as step 2 of the procedure for DDBD in the transverse direction using the direct procedure.

Step 3. Computing ductility demand and equivalent damping

The same as step 3 of the procedure for DDBD in the transverse direction using the direct procedure.

Step 4. Determining the effective period, secant stiffness and required strength

The same as step 4 of the procedure for DDBD in the transverse direction using the direct procedure.

Step 5. Checking the assumed strength distribution

If the bridge has abutments with known strength, the assumed values of v_l and v_n , must be verified. New refined values for v_{rl} and v_{rn} can be computed with Eq. 52 and Eq. 53. An error between the new and assumed values can be computed with Eq. 47 and Eq. 48.

$$v_{rl} = \frac{K_{eff,l}}{K_{eff}} \quad (\text{Eq. 52})$$

$$v_{rn} = \frac{K_{eff,n}}{K_{eff}} \quad (\text{Eq. 53})$$

If errors ER_{v_l} and ER_{v_n} and ER_{dp} are greater than a predefined tolerance, the procedure must be repeated from Step 2 the number of times required to get the errors within the tolerance. In each iteration the proportion of base shear taken by the abutments must be updated (i.e. $v_l = v_{rl}$, $v_n = v_{rn}$)

3.7 Concurrent orthogonal excitations

Real earthquakes induce three dimensional displacements with two horizontal components that could cause damage in the earthquake resisting components of the bridge. For this reason, DDBD must be applied in the two principal directions of the bridge and the results must be combined to produce a design capable of performing satisfactorily when attacked

in any direction. Strength demands along principal directions can be combined using the well known 100%-30% rule, currently used most seismic design codes (Imbsen, 2007; Caltrans, 2006). Application of this rule is presented in the following section.

3.8 Element Design

3.8.1 Pier design

The design of piers is based in Capacity Design principles to assure that all inelastic behavior take place in well detailed sections. The flexural design of reinforced concrete circular pier columns requires knowledge of moment, axial force and design concrete strain in the critical section of the element. The moments in the transverse, M_t , and longitudinal direction, M_l , are given by Eq. 54 and Eq. 55, in terms of the design shear that resulted of the application of DDBD, the shear height given by Table 3 and the number of columns in the pier, n_c .

$$M_t = \frac{V_t H_{st}}{n_c} \quad (\text{Eq. 54})$$

$$M_l = \frac{V_l H_{sl}}{n_c} \quad (\text{Eq. 55})$$

The 100%-30% rule for combination of forces caused by concurrent orthogonal combinations can be used to determine the design moment, M_E . In which case M_E is the grater of the two combinations of transverse M_t and longitudinal M_l moment demands given by Eq. 56 or Eq. 57.

$$M_E = \sqrt{M_t^2 + 0.3M_l^2} \quad (\text{Eq. 56})$$

$$M_E = \sqrt{M_l^2 + 0.3M_t^2} \quad (\text{Eq. 57})$$

The axial load P_G comes from a dead load analysis. The design strain ϵ_D must be reached when M_E is developed in the section. When designing for minimal or moderate inelastic actions, ϵ_D can be taken as 0.003 for nominal strength. When designing for the damage-

control or life-safety limit states, ε_D is taken as the least of the strains calculated in the critical section at the transverse or longitudinal design displacement. The strain ε_D is given by Eq. 58.

$$\varepsilon_D = \left(\frac{\Delta - \Delta_y}{L_p H_p} + \phi_y \right) c > 0.003 \quad (\text{Eq. 58})$$

Once P_G , M_E and ε_D are known, the amount of flexural reinforcement is determined by section analysis. This analysis should be based on realistic material models and expected rather than specified material properties. In practice, a moment-curvature analysis program could be used to determine by iteration the amount of flexural reinforcement required.

The shear design is based on a demand capacity analysis. The shear demand is based on the flexural over-strength of the section and must be computed in the design direction with the least shear height (H_s). The shear demand is given by Eq. 59, where Φ is an over-strength factor and H_s is the shear height given in Table 3 for different types of piers. If strain hardening was considered in the flexural design, $\Phi = 1.25$ is appropriate (Priestley et al, 2007). The shear capacity of the section can be determined using the modified UCSD model (Kowalsky and Priestley, 2000).

$$V_D = \frac{\Phi M_E}{H_s} \quad (\text{Eq. 59})$$

Combination of seismic and non-seismic loads

Element design in DDBD aims to provide the required strength to the earthquake resisting system so the design objective is met. The resulting structure should be capable of resisting gravity loads, other non-earthquake actions and the design earthquake attacking in any direction. Design for non-earthquake loads should follow LRFD practice specified by AASHTO (2004).

When designing piers in DDBD, it is not generally necessary to combine seismic with non-seismic moment demand. It is also not generally necessary to consider the axial loads generated by the earthquake. The reason is that combining seismic with non-seismic

moment and accounting for earthquake induced axial forces might lead to unnecessary over-strength in the structure.

For example, if the columns in the bent shown in Fig. 18a are only designed for gravity axial loads P_G and earthquake moments M_E , the strength developed by the bent in a Pushover analysis (Fig. 18b) will match the design strength V . If the seismic induced axial loads P_E are considered, the windward column, with less axial load, requires more reinforcement. However due to seismic reversal, the two columns must be provided with the same reinforcement, causing the bent to have more lateral strength than required, as shown in the pushover curve in Fig. 18b. If gravity load moments are included, the moment demand on the leeward column is increased, increasing also the amount of required reinforcement. Due to seismic reversal, the two columns should be detailed with the same amount of reinforcement, although only one really needs that much strength. The excess of reinforcement in one column, as in the previous case, causes unnecessary over-strength.

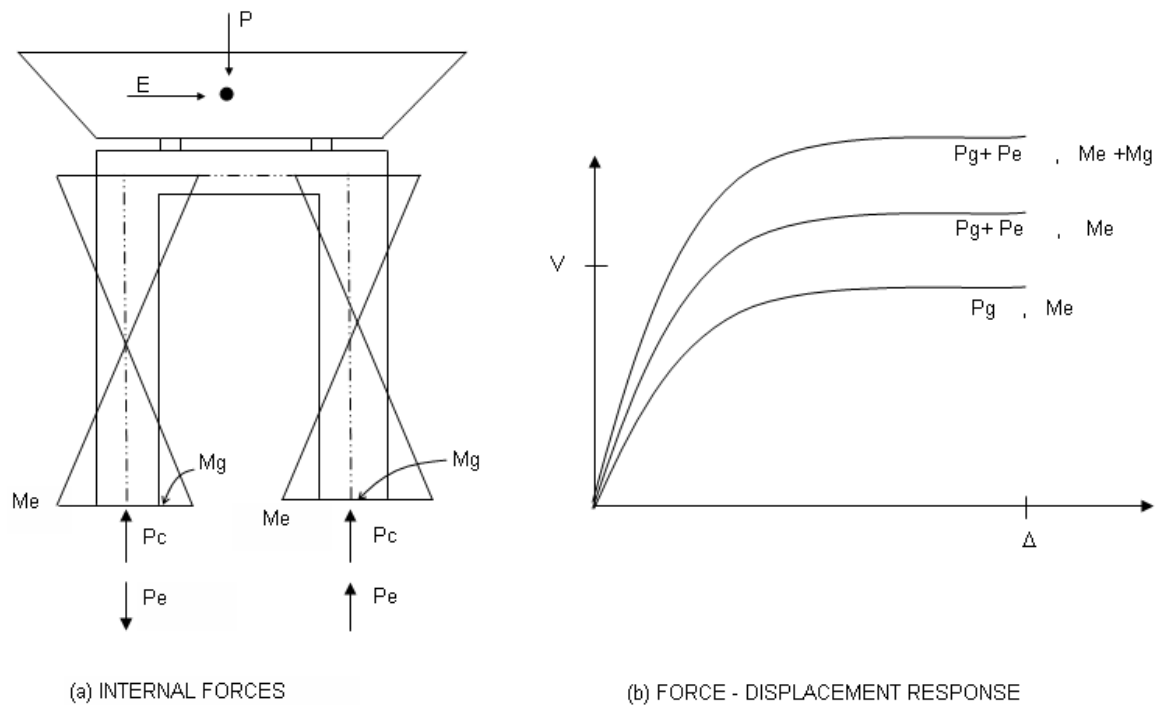


Figure 18 – Force-displacement response of bents designed for combinations of seismic and non-seismic forces.

Lateral over-strength is believed to be unnecessary unless it is required to accommodate non-seismic loads. For the example presented previously, if the columns are designed for M_E and P_G only, after the unavoidable gravity loads act, the lateral capacity of one column is reduced while the capacity of the other column is increased. Under lateral loading, one column might experience more damage than the other; however the overall response of the bent will be as planned. In the other hand, if the bent has over-strength in an attempt to limit the damage in a critical section of the bent, due to the over-strength, the bent will have a conservative response and not even the critical section will reach the design limit state, which is thought to be uneconomical.

The arguments presented above apply to all design situations where the gravity loads produce moments that increase the lateral capacity of some columns and reduce the capacity of others. No consideration of gravity moments and seismic induced axial forces is especially appropriate for cases where design is controlled by $P-\Delta$ effects rather than damage-based limit states. Caution must be exercised in the case of curved bridge frames with integral single column piers, where gravity loads reduce the lateral capacity of all columns. Seismic axial loads should not be ignored in columns with high axial load ratios, where additional axial loads could lead to brittle failures.

3.8.2 Abutment design

The effects that the abutments have in the response of the bridge depend on their contribution of strength and stiffness. Seat-type abutments have sacrificial shear keys and knock off walls and generally contribute little to the strength of the bridge. Integral abutments are monolithic with the superstructure and must be strong enough to restrain superstructure displacement and avoid excessive damage. DDBD can be used to obtain the design actions for these types of abutments, as explained next:

Integral Abutments

Generally, abutments have less displacement capacity than the adjacent bents. Therefore, integral abutments must be effective in restraining the displacement of the superstructure at

their ends to avoid excessive damage. To do this, integral abutments must be strong and stiff.

To design integral abutments with DDBD, the designer specifies, a maximum displacement to be reached by the abutments in the in-plane and out-of-plane directions. The designer must also specify the amount of viscous damping and a skew angle if any. The amount of damping should be between 5 and 10%, as recommended by AASHTO (Imbsen, 2007) for continuous bridges, in which there is considerable soil mobilization at the abutments. If plastic hinges are expected to develop in the supporting piles, the amount of viscous damping could be further increased as a function of ductility demand (See section 2.1).

Continuous bridges with integral abutments are expected to respond in the transverse direction with a flexible displacement pattern. The shape of the pattern is unknown before design and is generally given by the first mode of vibration. Therefore DDBD is applied with the FMS algorithm or the EMS algorithm (Table. 2) (see Section 3.5).

If the target displacement is less than their yield displacement, the abutments will perform elastically during the earthquake. If that is the case, it is important to consider the additional demands generated by higher modes of vibration. Such determination can be accomplished using the EMS algorithm or by the application of a dynamic amplification factors. Analyses performed by the authors on a set of ten bridges with integral abutments, showed that the shear demand in the abutments can be increase up to 2.5 times the forces derived from the FMS design (Suarez and Kowalsky, 2008a)

The application of DDBD in the longitudinal direction is direct for bridges with integral type of abutments. The ratio of the total base shear taken by the abutments can be decided by the designer at the beginning of design.

Seat type abutments

This type of abutments are typically designed for non-seismic loads and protected from seismic demands by the provision of sacrificial shear keys and knock off walls that are designed to fuse. In the in-plane direction, contribution to the strength of the bridge is given by passive pressure of the soil that is mobilized behind the wing walls and residual strength or friction after the shear keys fail. In the longitudinal direction, the strength contribution comes from passive pressure of the soil mobilized behind the back-walls that is compressed. Methods for determining the strength and yield displacement of these elements are well known and presented in detail in AASHTO Guide Specification for LRFD Seismic Bridge Design (Ibsen, 2007).

When designing a continuous bridge with seat-type abutments, their contribution to the strength and the effect on the response of the bridge can be easily accounted for in DDBD. The force-displacement response of the abutment must be known in both direction of design. In this case, DDBD will limit the response of the abutment to the specified target displacement by allocating the appropriate level of strength in the bridge piers. Since the ratio of the total base shear taken by the abutments is not known at the beginning design, DDBD requires iteration. The study of higher mode effects is unnecessary for elasto-plastic abutments since demand cannot exceed capacity.

4. COMPUTERIZATION OF DDBD

The computer program DDBD-Bridge has been developed for automation of the DDBD method for highway bridges. In most design cases DDBD can be applied with manual or spreadsheet calculations using the direct procedure. However, time in the application of the FMS or EMS algorithms and section design could be saved by programming the algorithms into a computer code.

DDBD-Bridge has been programmed following the general procedure presented in this report. The program has the following features:

- DDBD of highway bridges in the transverse and longitudinal directions
- Design using the direct, FMS and EMS algorithms

- Continuous superstructures or superstructures with expansion joints
- Integral or seat-type abutments
- All types of piers shown in Table 3
- Automated section design by moment-curvature analysis

The program and its documentation can be accessed and used on-line through the Virtual Laboratory for Earthquake Engineering (www.utpl.edu.ec/vlee) (Dr. Kowalsky, this URL will be available starting on July 8)

4.1 DDBD using commercially available structural analysis software

Any frame analysis program capable of performing static and response spectrum analysis can be used to perform the Step 3 of the FMS or EMS algorithms presented in Section 3.5.

Even though static analysis is not required in the direct solution (Section 3.5.1.), inertia forces can be calculated (Eq. 44) and applied to an elastic model of the bridge to get element forces and easy element design. This is equivalent to apply the FMS algorithm (Section 3.5.2) without iteration.

When applying the iterative design algorithms, the secant stiffness of the elements must be updated in the model in each iteration. If a 3D model is used with the piers modeled using frame elements, Eq. 60 can be used to compute inertia reduction factors, I_{rf} , for each element. In this equation, E is the elastic modulus used in the analysis program, I_g is the gross moment of inertia of the section and γ is 1/3 for pinned head columns and 1/12 for fixed head columns. Inertia reduction factors are accepted in most analysis programs to modify the gross section properties of frame elements.

$$I_{rf} = \frac{K_i H^3}{\gamma E I_g} \quad (\text{Eq. 60})$$

4.1 Evaluation of DDBD with Inelastic Time History Analysis

Inelastic Time History Analysis (ITHA) is considered to be the most accurate tool to assess structural performance. Other assessment methods based on nonlinear static analysis (Pushover) such as the Capacity Spectrum Method (FEMA, 2005) or the Displacement Coefficient Method (FEMA, 2005) should not be used for assessment of structures designed with DDBD since these methods also use equivalent linearization and an assumed pattern of displacement. Therefore, there is no reason to believe that the performance predicted by assessment methods based on Pushover analysis is more accurate than the target performance used in DDBD.

Research on DDBD of bridges (Kowalsky, 2002; Dwairi and Kowalsky, 2006; Ortiz, 2006; Suarez and Kowalsky, 2008a) has shown good agreement between the target performance used in DDBD and the performance simulated by ITHA. This has proven that DDBD is an effective design method and therefore, in general, designs done with DDBD do not require evaluation by ITHA or other method. Exemptions to this are the cases where the bridges have characteristics that cannot be captured by DDBD or have not yet been studied for their implementation in DDBD. Additionally, ITHA may be required by the owner for important/essential bridges. The conditions under which ITHA may be required for design evaluation are:

- Bridges with more than six spans
- Bridges with more than two internal expansion joints in the superstructure
- Curved bridges where the subtended angle is greater than 90°
- Highly irregular configurations
- When the target displacement and target ductility of critical components cannot be accurately assessed. This may happen for some substructures that are not considered in Table 3 or for drilled shaft bents when soil conditions are different of those assumed for the definition of the equivalent model

The program ITHA-Bridge has been developed to perform ITHA of highway bridges. This program is a pre-processor and post-processor of OpenSees (Mazoni et al, 2006) and has the following features:

- From a basic input automatically generates the bridge model files for OpenSees.
- Supports the substructures shown in Table 3, integral and seat-type abutments. Also supports superstructure joints and plan curvature.
- Multiple acceleration records can be run in batch mode automatically.
- Checks convergence errors in solution and adjusts the analysis time step if necessary to achieve convergence.
- Produces and output file combining the output of the different acceleration records that were run.

ITHA-Bridge and its documentation can be accessed and used on-line through the Virtual Laboratory for Earthquake Engineering (www.utpl.edu.ec/vlee).

5. APPLICATION EXAMPLES

5.1 Superstructure target displacement

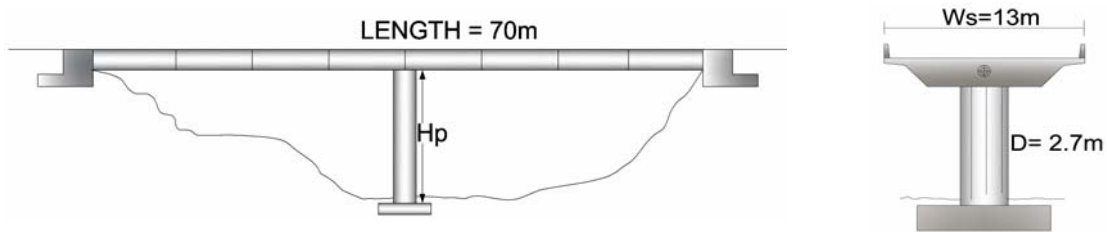


Figure 19 – Two span continuous bridges

This example illustrates the effect of superstructure displacement capacity in the ductility of the central pier of the bridge shown in Fig. 19. It is assumed that the displacement capacity of the continuous superstructure is controlled by the yielding of the longitudinal reinforcement in the concrete deck. The yield displacement of the superstructure is computed at the location of the central pier. The length of the bridge is $L_s = 70$ m and the width of the superstructure deck is $w_s = 13$ m, as shown in Fig. 19.

$$\mu_{\Delta i} = \frac{\Delta_{ysi}}{\Delta_{ypi}} \quad (\text{Eq. 61})$$

The ductility of the central pier is computed with reference to the yield displacement of the superstructure using Eq. 61, for a range of pier heights H_p . The yield displacement of the superstructure computed with Eq. 14 is $\Delta_{ys2} = 0.207$ m. This is based on $\Delta_1 = \Delta_3 = 0.05$ m. The yield displacement of the central pier, Δ_{yp2} , is computed with Eq. 20. The yield curvature of the superstructure is computed with Eq. 10 and the yield curvature of the pier is computed with Eq. 19. In both cases the yield strain of steel is $\varepsilon_y = 0.002$.

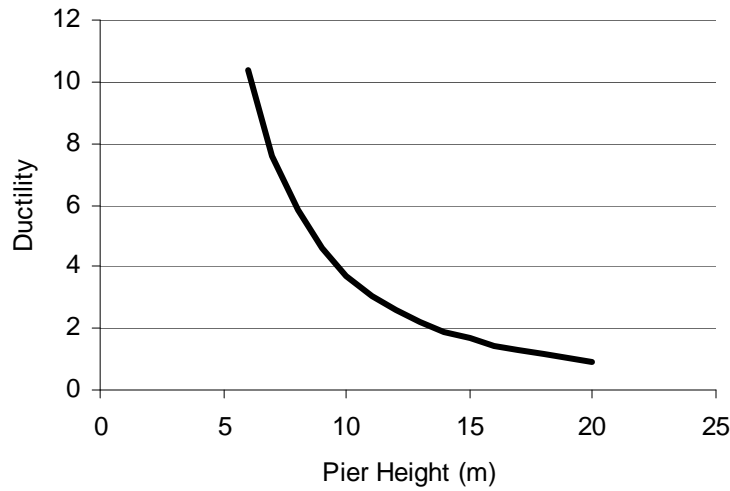


Figure 20 – Target ductility of central pier of two span bridge

If the height of the pier H_p is varied from 6 m to 20 m, the target ductility of the pier, limited by target displacement of the superstructure, varies as shown in Fig. 20. Well confined piers designed for the life-safety limit state have a target ductility of 6 (See section 3.1). Therefore, if the height of the central pier is greater than 10 m, the target displacement of the pier is governed by the yield displacement of the superstructure rather than by target displacement of the pier itself. If the pier is 20 m tall, the yield displacement of the pier equals the yield displacement of the superstructure.

5.2 Stability-based target displacement model

To assess the effectiveness of the proposed model, Eq. 25 was used in the single column pier shown in Fig. 21, to find the target ductility to meet a stability index, $\theta_s = 0.3$. The diameter of the reinforced concrete column is 1.8 m. The axial load is $P = 6107$ kN and the mass is $M_{\text{eff}} = 622.5$ t. The height of the column is varied between 5.4 m and 27 m so the aspect ratio ranges from 3 to 15. The pier is designed for a displacement spectra with $T_c = 3.5$ s and the $PSD = 0.71$ m. The results are presented in Fig. 22

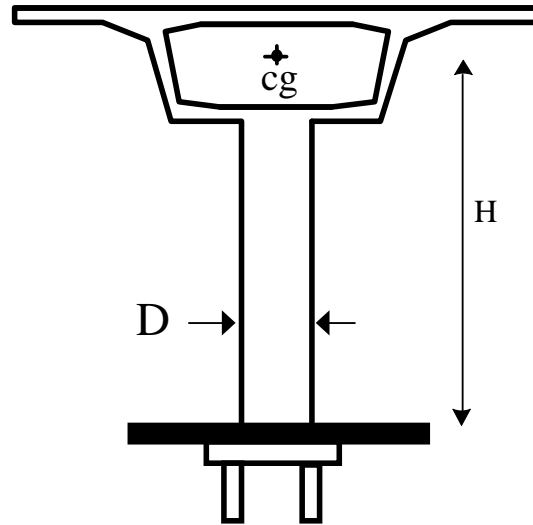
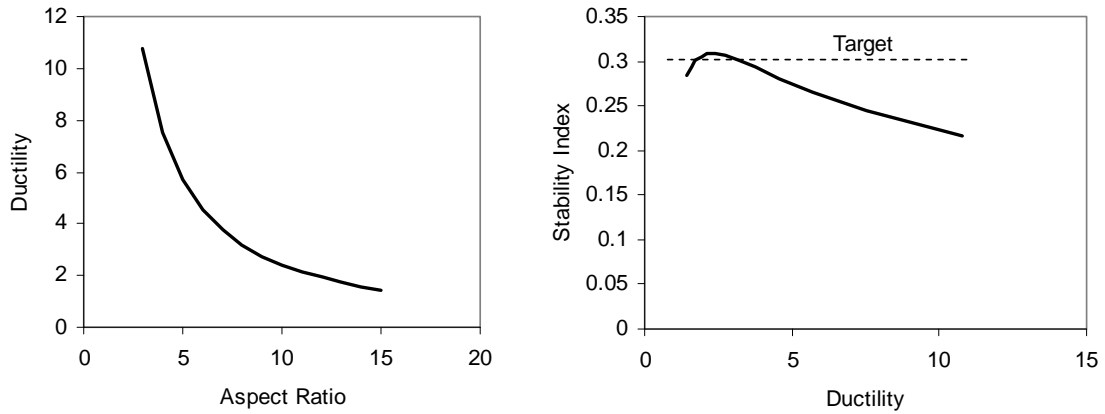


Figure 21 - Single Column Bent

Results in Fig. 22a indicate that the target ductility reduces fast when the aspect ratio increases. If the life-safety ductility for the pier is six, $P-\Delta$ controls design when the aspect ratio is higher than five.

Continuing design, using the stability-based ductility as target ductility, $P-\Delta$ effects are checked at the end and θ_s can be plotted against ductility as shown in Fig. 22(b). This figure shows that the proposed model can effectively predict the target ductility to meet the specified stability index.



(a) Ductility vs. Aspect Ratio

(b) Stability index vs. Ductility

Figure 22 - Stability based ductility vs. aspect ratio for a single column pier

5.3 Skewed bent design

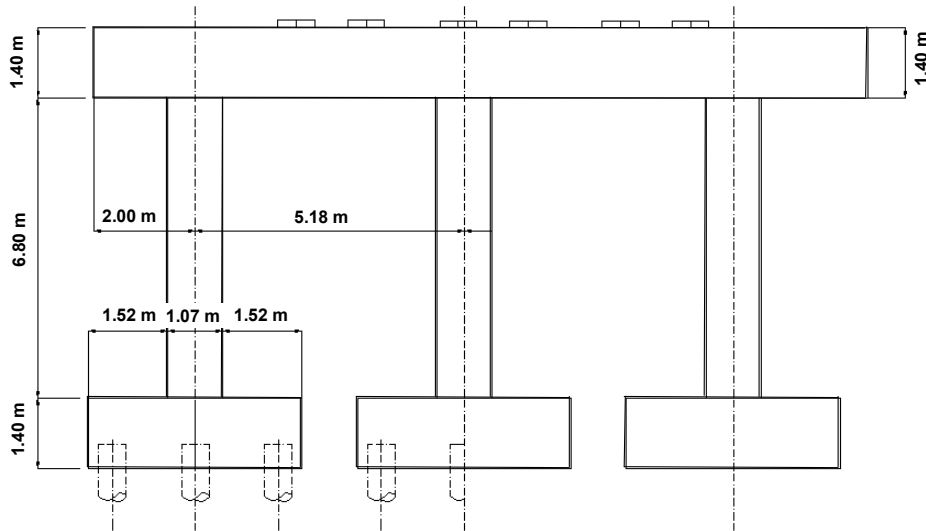


Figure 23 - Multi column bent

The multi column bridge bent shown in Fig. 23 was designed with 0, 15, 30 and 45 degrees of skew. Once designed, the performance of the bent was assessed by ITHA. This multi-column bent supports simply supported spans of a highway bridge. The tributary weight of the superstructure is 6408 kN, the weight of the cap-beam is 562 kN. The bent has three circular, 1.05 m diameter, reinforced concrete columns, with height equal to 6.80 m. The

height of the cap-beam is 1.37 m. To meet detailing requirements regarding to minimum reinforcement and spacing, the columns are reinforced with longitudinal bars of 25 mm and hoops of 13 mm spaced 150 mm. $f'_{ce} = 34.45$ MPa, $\epsilon_y = 0.0022$, $\epsilon_{su} = 0.06$, $f_{yh} = 414$ MPA.

The bent was designed to meet the damage control limit state under the earthquake represented by the displacement spectrum shown in Fig. 24, where $T_c = 3.5$ s and the $PSD = 0.71$ m. The damage-control concrete compression strain computed with Eq. 7 is $\epsilon_{dc} = 0.017$. The damage control displacement of the bent is $\Delta_{T,in} = 146$ mm in the in-plane direction and $\Delta_{T,out} = 317$ mm in the out-of-plane direction. These values were calculated with Eq. 16 with reference to Table 3. The yield displacement is $\Delta_{y,in} = 43$ mm in the in-plane direction and $\Delta_{y,out} = 115$ mm in the out-of-plane direction. These values are computed with Eq. 20, with reference to Table 3. The effective height of the bent is $H_{p,in} = 6.8$ m in the in-plane direction and $H_{p,out} = 8.17$ m in the out-of-plane direction.

Using Eq. 23 and Eq. 24, the in-plane and out-of-plane design parameters are projected in the transverse and longitudinal directions of the bridge for the different skew angles. The results are presented in Table 6.

Table 6 - Design parameters from local to global axes

Skew	Δ_t (mm)	Δ_l (mm)	Δ_{yt} (mm)	Δ_{yl} (mm)	H_t (m)	H_l (m)
0	146	317	43	115	6.8	8.17
15	174	288	55	103	7	7.94
30	203	260	67	91	7.26	7.71
45	231	231	79	79	7.49	7.49

For each target displacement in the transverse and longitudinal directions, design was continued to get the required strengths V_t and V_l and design moments M_t and M_l . Finally the amount of longitudinal reinforcement was obtained by section analysis using the axial load and the combined moment M_E . This process was done as explained in Section 3.8. The design results are summarized in Table 7, where ρ is the longitudinal steel ratio required in the section.

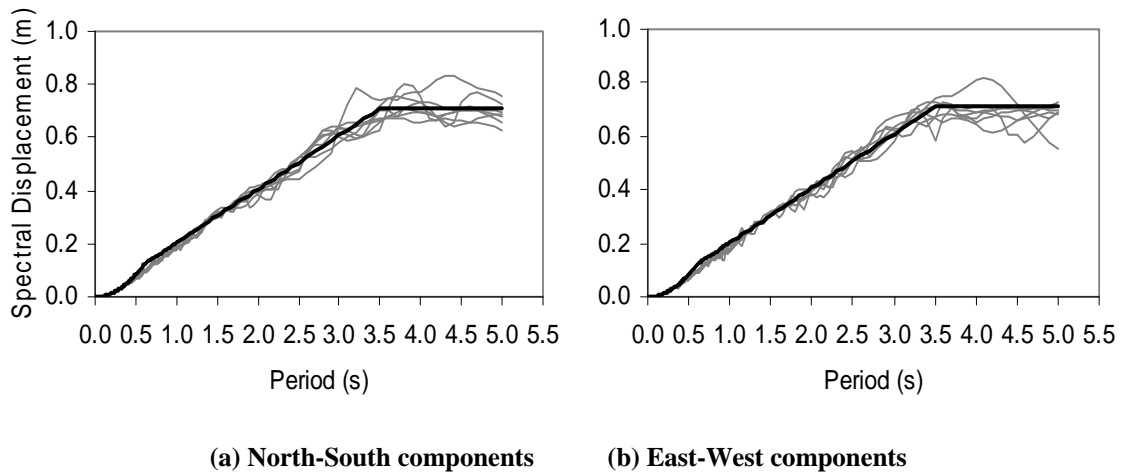
Table 7 - Design results for multi-column bent

Skew	V_t (kN)	V_l (kN)	M_t (kN.m)	M_l (kN.m)	M (kN.m)	ρ %
0	3341	1624	3786	4423	4566	2.61
15	2840	1776	3327	4702	4807	2.83
30	2470	1959	2987	5039	5118	3.06
45	2185	2185	2726	5453	5514	3.4

It is observed in Table 7 that as the skew increases, the displacement capacity in the longitudinal direction decreases. This causes the strength demand in that direction to increase. The required reinforcement also increases and since design is controlled by response in longitudinal direction.

To assess the response of the skewed bent, ITHAs were conducted using OpenSees (Mazzoni et al, 2005). The columns were modeled using fiber sections, with nonlinear stress-strain models for reinforcing steel, confined and unconfined concrete. The cap-beam was modeled with elastic frame elements.

Six finite element models were built. Three models had skew angles of 15° , 30° and 45° , but the columns were reinforced as for 0 skew. The other models had the different skew angles and the reinforcement required for each level of skew. All models were subjected to the two horizontal components of the seven earthquake compatible records shown in Fig. 24.

**Figure 24 - Displacement spectrum and displacement spectra of 7 earthquake compatible records**

During the displacements in the local axes of the bent were recorded at the time in which maximum concrete strains were reached. These results were averaged with results from the other records. The final results are presented in Table 8. It is observed that the response in longitudinal direction controls design in all cases. In the models were the reinforcement was not increased with skew, the demand increases as the skew increases. In the models were the reinforcement was increased with skew, the demand was maintained. It is concluded then, that the proposed method is capable of capturing the effects of skew in this types of bents.

Table 8 - Design results for multi-column bent

Skew	Design for 0 skew		Designed for skew	
	Δ_{in} (mm)	Δ_{out} (mm)	Δ_{in} (mm)	Δ_{out} (mm)
15	32	264	17	250
30	29	276	15	269
45	28	297	16	256

5.4 DDBD of a three span continuous bridge with seat-type abutments

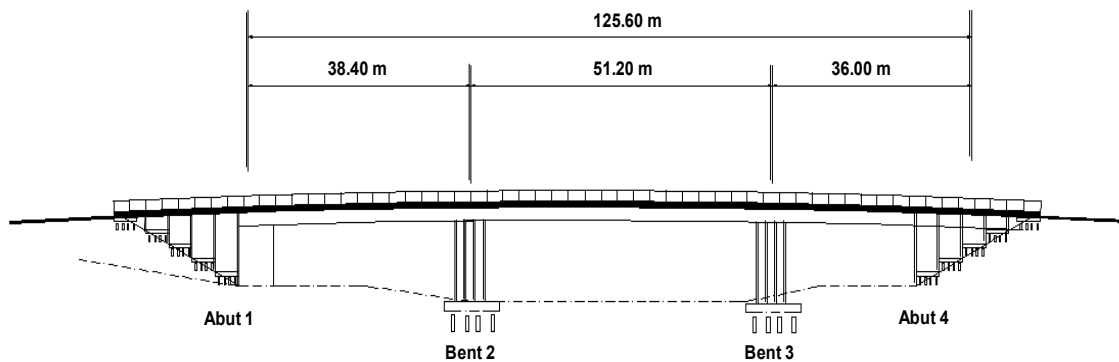


Figure 25 - Elevation view three span bridge

This bridge has three spans of 38.41 m, 51.21 m and 35.98 m respectively and a total length of 125.60 m. The superstructure is a continuous prestressed reinforced concrete box girder. The two bents have two 1.83 m diameter columns supported on piles. Column

height varies from 13.40 m at bent two to 14.30 m at bent three. The columns are pinned at the bottom and fixed to an integral bent in the superstructure. The abutments are seat type with brake-off walls. An elevation view of the bridge is presented in Fig. 25 and the superstructure section and substructure configuration are shown in Fig. 26. The reinforced concrete in piers has the following properties: $f'_{ce} = 36$ MPA, $f_{ye} = 455$ MPA, $\varepsilon_y = 455/200000 = 0.0022$, $\varepsilon_{su} = 0.1$, $f_{yh} = 414$ MPA.

The seismic hazard at the bridge site is given by the design spectra, with 5% damping, shown in Fig. 27. The corner period of the displacement spectra is 8 s (FEMA, 2003), and the maximum spectral displacement is 1.92 m.

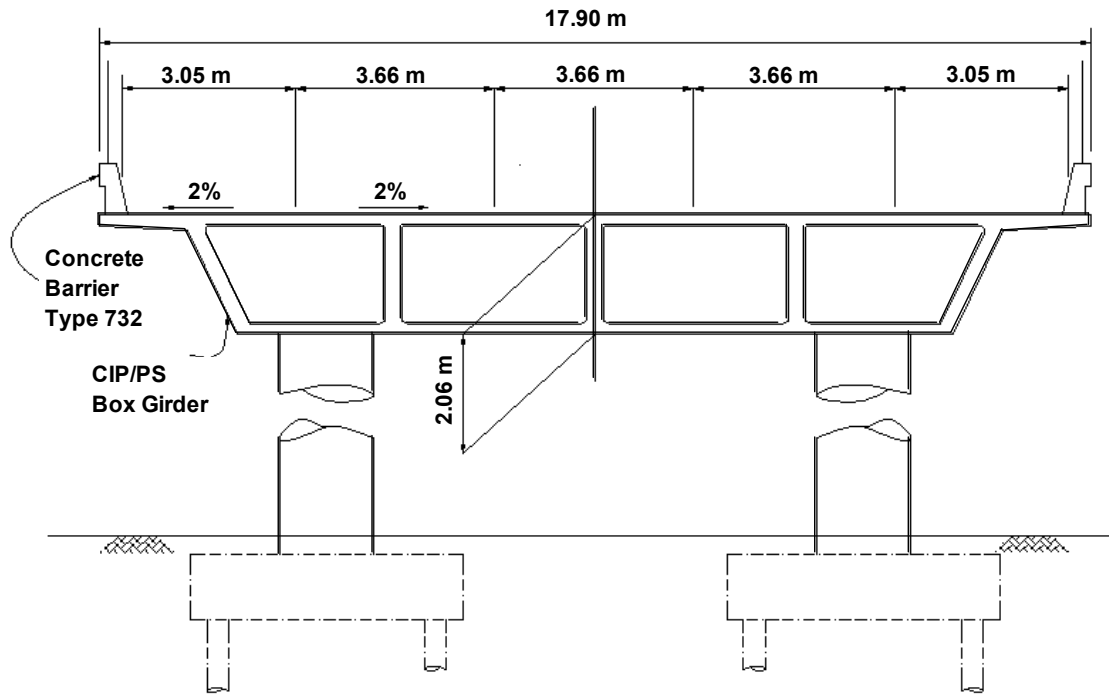


Figure 26 - Superstructure section and interior bent

Design Objective

Under the design earthquake represented by the displacement spectra shown in Fig. 27, the bridge shall meet one or more of the following performance limits: 1) damage control strains in the columns, 2) stability index less than 30%

Assessment of Target Displacement

Complying with min reinforcement requirements of AASHTO (Imbsen, 2007), D44 longitudinal bars and a D25 spiral spaced 130 mm are chosen for the columns.

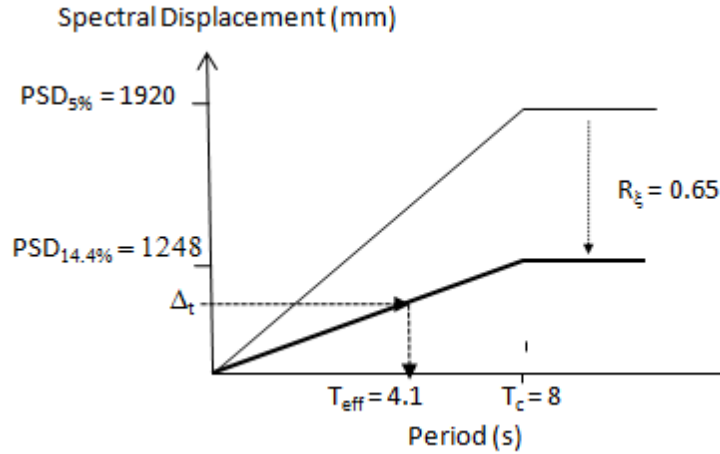


Figure 27 – Displacement Spectra

1. The damage control displacement Δ_{DC} of the bents is determined with the plastic hinge method (Eq. 16), assuming single bending in the columns. These calculations are valid for the two directions of design. The yield displacement Δ_y (Eq. 20) and damage-control displacement Δ_{DC} are shown in Table 9. The damage control compression strain for concrete is $\epsilon_{c,dc} = 0.018$ and controls the determination of Δ_{DC} .
2. The stability based target displacement is computed with Eq. 25 and Eq. 26. The results are shown in Table 9. It is observed in this table that stability-based displacement controls design and becomes target design displacement.

Table 9 - Target displacements Trial design CA-1

	H (m)	D (m)	P (kN)	Δ_y (m)	Damage Control Δ_c (m)	P- Δ Δ_c (m)
Bent 2	13.4	1.83	6714	178	656	640
Bent 3	14.3	1.83	6557	202	737	650

Strength Distribution.

The strength is be distributed among the bents so that all columns have the same reinforcement (See Section 3.5). The proportion of the total base shear taken by each bent in computed with Eq. 31, assuming that the abutments will contribute 10% of the total strength in the transverse and longitudinal directions (i.e. $v_s = 0.1$ in Eq. 31). Applying Eq. 31 it is found that $v_2 = 0.46$ and $v_3 = 0.44$

Design in Transverse Direction

Design in the transverse direction will account for interaction between the superstructure, bents and abutments. The superstructure section shown in Fig. 26 has an out-of-plane inertia $I = 222 \text{ m}^4$, an elastic modulus $E_s = 26500 \text{ MPa}$, and a weight $W_s = 260 \text{ kN/m}$.

The abutments are assumed to have an elasto-plastic response. The transverse strength or yield force of the abutments is computed considering there are sacrificial shear keys that will brake during the design earthquake. The residual strength in the abutment comes from friction between the superstructure and the abutment. Assuming a friction coefficient of 0.2, with a normal force equal to the tributary superstructure weight carried by the abutments, the transverse strength of the abutments is 1300 kN. It is assumed that the yield displacement is 50mm.

Step 1. Target displacement profile. Since the bridge is regular and the superstructure is stiff, the abutments are not expected to restrain the displacement of the superstructure and a rigid body displacement patter will be used (Section 3.4.1) (Suarez and Kowalsky, 2008a). As a result of this, all substructures displace the same amount and the amplitude of the displacement profile is given by the bent 2, which is the one with the least target displacement (Table 12).

Step 2. Equivalent single degree of freedom system. With the bents and abutments displacing the same amount in the transverse direction Eq. 1 and Eq. 2 reduce to Eq. 62 and Eq. 63. The generalized displacement equals the target design displacement of bent 2

so $\Delta_{sys} = 640$ mm. Also the effective mass of the bridge is the sum of the total mass of the superstructure, integral bent-caps and one third of the weight of the columns, $M_{eff} = 3808$ t.

$$\Delta_{sys} = \Delta_T \quad (\text{Eq. 62})$$

$$M_{eff} = \sum_{i=1}^{i=n} M_i \quad (\text{Eq. 63})$$

Step 3. Equivalent damping. The ductility at the target displacement level is $\mu_1 = 12.80$, $\mu_2 = 3.59$, $\mu_3 = 3.16$, $\mu_4 = 12.80$. These values are obtained as ratios between Δ_{sys} and the yield displacement of each substructure. Equivalent damping is computed for each bent as a function of ductility using Eq. 3. Assuming the abutments respond with 10% of critical damping, $\xi_1 = 10\%$, $\xi_2 = 15.2\%$, $\xi_3 = 14.7\%$, $\xi_4 = 10\%$. The damping combined with Eq. 36 in terms of work done by each element, results in $\xi_{sys} = 14.4\%$.

Step 4. Required strength. The level of damping in the bridge results in a displacement demand reduction factor $R_\xi = 0.65$ (Eq. 37). As shown in Fig. 27, by entering the reduced displacement spectrum with Δ_{sys} , the required period is $T_{eff} = 4.1$ s (Eq. 38). Finally, the required strength for the bridge in the transverse direction is $V = 5700$ kN (Eq. 40).

Step 5. Checking assumed strength distribution. Since the abutments yield at 50 mm, at the target displacement, both abutments develop their full strength, $V_a = 2600$ kN. Therefore the proportion of the total strength taken by the abutments is $v_a = 2600/5700 = 45\%$ (Eq. 42). This is 4.6 times the value assumed at the beginning of the process, therefore ξ_{sys} must be re-evaluated to obtained a new V . After a few iterations $V = 6447$ kN and the participation of the abutments is 39 %, as shown in Table 10.

It is important to note that iteration was required since it was chosen to consider the strength of the abutments. Accounting for the strength of the abutments has significantly reduced the demand on the piers. However whether the abutments are able to contribute this strength after several cycles of displacements as large as 0.6 m might be questioned.

Table 10 - Transverse design parameters

Iteration	Δ_{sys}	M_{eff}	ξ_{sys}	T_{eff}	V	$(V1+V4)/V$
1	0.64	3808.1	14.4	$>T_c$	5879.8	0.1
2	0.64	3808.1	13.3	3.9	6313.3	0.45
3	0.64	3808.1	13.1	3.87	6417.2	0.38
4	0.64	3808.1	13	3.86	6447.8	0.39

Longitudinal Direction

The design process along the longitudinal direction is similar to design in transverse direction. Since the columns are pinned to the foundation and they are integral with the superstructure, the target displacement in the longitudinal direction is the same as the target displacement in the transverse direction. Also, since the superstructure is stiff and continuous, the displacement at the location of the bents and abutments are constrained to be the same. Therefore, Δ_{sys} and M_{eff} are the same as in transverse direction.

Since the longitudinal direction the abutments are designed with knock-off walls, their strength comes from soil mobilization behind the wall pushed by the superstructure. For a wall 14 m wide and 2.5 m tall, assuming a passive pressure of 70 kPa/m (Imbsen, 2007), the strength of the backfill is 6080 kN. Also, using Eq. 15, the yield displacement can be taken as 75 mm. An elasto-plastic compression only response based on these values is used for this design. The equivalent damping of the abutments is assumed constant, equal to 10%

Table 11 - Longitudinal design parameters

Iteration	Δ_{sys}	M_{eff}	ξ_{sys}	T_{eff}	V	$(V1+V4)/V$
1	640	3808.1	14.5	$>T_c$	5699.9	0.1
2	640	3808.1	11	3.69	7247.1	0.8
3	640	3808.1	10.8	3.66	7349.5	0.84
4	640	3808.1	10.9	3.67	7316	0.82

Table 11 summarizes the values of the parameters for longitudinal design. A few iterations were required as it was found that the abutments contribute with as much as 82% of the total strength in this direction. In the first iteration, it was assumed that the contribution of

the abutments was 10%. This yielded a total required strength of 5699 kN, which is actually less than the capacity of the abutment that resist the movement of the superstructure. Therefore that solution is not possible. Repeating the process but starting with 80% as abutment contribution, increases the strength demand since the damping is reduced. After three iterations the solution converges, $V = 7316$ kN and the contribution of the abutments is 82%.

Element Design

In DDBD, the flexural reinforcement is designed using moment-curvature analysis to provide the required strength at a level of curvature compatible with the ductility demand in the element. Table 12 shows the design moments in the transverse M_t and longitudinal direction M_l that resulted from DDBD. It is observed that these values are the same for bents 2 and 3, as it was chosen in the strength distribution. These values are followed by the combined moment M_E . This resulted from the largest of the values obtained with Eq. 56 and Eq. 57, using the 100%-30% combination rule.

Table 12 – Element design parameters

BENT	M_T (kN.m)	M_L (kN.m)	$M_{t\ P-\Delta}$ (kN.m)	$M_{l\ P-\Delta}$ (kN.m)	θ_t	θ_l	M_E (kN.m)	P (kN)	ρ (%)	Shear D/C ratio
2	14975	4446	4408	4408	0.29	0.29	17238	7547	1.1	0.24
3	14975	4446	4304	4304	0.29	0.29	17238	7547	1.1	0.25

Also shown in Table 12 are the P- Δ moments in the transverse P- Δ_t and longitudinal P- Δ_l direction along with the stability indexes calculated as the ratio of the P- Δ moments and the combined moment. In DDBD the stability index should be less than 30%. However, if the stability index is larger than 8%, the design moment must be increased adding 50% of the P- Δ moment to account for strength reduction caused by P- Δ effects (Priestley et al, 2007). These increased moments are shown in Table 12 along with the design axial force, P, that results from gravity loads only.

At the design displacements, the strain in the concrete reaches values of 0.011 for bent 2 and 0.010 for bent 3 (Eq. 58). By section analysis at the design strains, it is found that all columns in the bridge require 20D44 bars as flexural reinforcement, which is a 1.1% steel ratio.

Finally, using the modified UCSD shear model (Kowalsky and Priestley, 2000), the shear capacity of the section is computed and compared to shear demand at flexural over-strength. The shear demand/capacity ratios are shown in Table 12. Since the shear demand capacity ratios are less than one, it is concluded that the amount of adopted shear reinforcement is conservative.

8. REFERENCES

- Caltrans, 2006a, Seismic Design Criteria, Caltrans, http://www.dot.ca.gov/hq/esc/earthquake_engineering, (accessed April 18, 2008)
- Caltrans, 2006b, LRFD Design Example B November 3, 2006 – Version 1.1, AASHTO, <http://cms.transportation.org/?siteid=34&pageid=1800>, (accessed April 18, 2008).
- Calvi G.M. and Kingsley G.R., 1995, Displacement based seismic design of multi-degree-of-freedom bridge structures, *Earthquake Engineering and Structural Dynamics* 24, 1247-1266.
- Dwairi, H. and Kowalsky, M.J., 2006, Implementation of Inelastic Displacement Patterns in Direct Displacement-Based Design of Continuous Bridge Structures, *Earthquake Spectra*, Volume 22, Issue 3, pp. 631-662
- EuroCode 8, 1998, Structures in seismic regions – Design. Part 1, General and Building”, Commission of European Communities, Report EUR 8849 EN
- Imbsen, 2007, AASHTO Guide Specifications for LRFD Seismic Bridge Design, AASHTO, <http://cms.transportation.org/?siteid=34&pageid=1800>, (accessed April 18, 2008).
- Kowalsky M.J., 2002, A Displacement-based approach for the seismic design of continuous concrete bridges, *Earthquake Engineering and Structural Dynamics* 31, pp. 719-747.

- Kowalsky M.J., Priestley M.J.N. and MacRae G.A. 1995. Displacement-based Design of RC Bridge Columns in Seismic Regions, *Earthquake Engineering and Structural Dynamics* 24, 1623-1643.
- Mander, J.B., Priestley, M.J.N. and Park, R., 1988a, Theoretical Stress Strain Model of Confined Concrete *Journal of Structural Engineering*, ASCE, Vol. 114, No.8, August, 1988
- Mazzoni, S., McKenna, F., Scott, M. and Fenves, G., 2004, OpenSees command language manual, <http://opensees.berkeley.edu>, (accessed April 18, 2008)
- Paulay, T, Priestley, M.J.N., 1992, *Seismic Design of Reinforced Concrete and Masonry Buildings*, Wiley, 978-0-471-54915-4
- Priestley, M. J. N., 1993, Myths and fallacies in earthquake engineering-conflicts between design and reality, *Bulletin of the New Zealand Society of Earthquake Engineering*, 26 (3), pp. 329–341
- Priestley, M. J. N., Calvi, G. M. and Kowalsky, M. J., 2007, *Direct Displacement-Based Seismic Design of Structures*, Pavia, IUSS Press
- Priestley, M. J. N., Verma, R., Xiao, Y., 1994, Seismic Shear Strength of Reinforced Concrete Columns, *Journal of Structural Engineering* 120(8) (1994) pp. 2310–2328
- Shibata A. and Sozen M. Substitute structure method for seismic design in R/C. *Journal of the Structural Division*, ASCE 1976; 102(ST1): 1-18.
- Suarez, V.A. and Kowalsky M.J., Displacement-Based Seismic Design of Drilled Shaft Bents with Soil-Structure Interaction, *Journal of Earthquake Engineering*, Volume 11, Issue 6 November 2007 , pp. 1010 – 1030
- Suarez, V.A., 2008, *Implementation of Direct Displacement Based Design for Highway Bridges*, PhD Dissertation, North Carolina State University.
- Veletsos, A. and Newmark, N. M., 1960, Effect of inelastic behavior on the response of simple systems to earthquake motions”, *Proceedings of 2nd World Conference on Earthquake Engineering*, pp. 895 – 912.